Am J Physiol Heart Circ Physiol 293: H2516–H2522, 2007.
First published July 20, 2007; doi:10.1152/ajpheart.00424.2007.

Angiotensin II attenuates myocardial interstitial acetylcholine release in response to vagal stimulation

Toru Kawada,[1] Toji Yamazaki,[2] Tsuyoshi Akiyama,[2] Meihua Li,[1,3] Can Zheng,[1,3] Toshiaki Shishido,[1] Hidezo Mori,[2] and Masaru Sugimachi[1]

[1]*Department of Cardiovascular Dynamics, Advanced Medical Engineering Center and* [2]*Department of Cardiac Physiology, National Cardiovascular Center Research Institute, Osaka; and* [3]*Japan Association for the Advancement of Medical Equipment, Tokyo, Japan*

Submitted 5 April 2007; accepted in final form 19 July 2007

Kawada T, Yamazaki T, Akiyama T, Li M, Zheng C, Shishido T, Mori H, Sugimachi M. Angiotensin II attenuates myocardial interstitial acetylcholine release in response to vagal stimulation. *Am J Physiol Heart Circ Physiol* 293: H2516–H2522, 2007. First published July 20, 2007; doi:10.1152/ajpheart.00424.2007.—Although ANG II exerts a variety of effects on the cardiovascular system, its effects on the peripheral parasympathetic neurotransmission have only been evaluated by changes in heart rate (an effect on the sinus node). To elucidate the effect of ANG II on the parasympathetic neurotransmission in the left ventricle, we measured myocardial interstitial ACh release in response to vagal stimulation (1 ms, 10 V, 20 Hz) using cardiac microdialysis in anesthetized cats. In a control group ($n = 6$), vagal stimulation increased the ACh level from 0.85 ± 0.03 to 10.7 ± 1.0 (SE) nM. Intravenous administration of ANG II at 10 $\mu g \cdot kg^{-1} \cdot h^{-1}$ suppressed the stimulation-induced ACh release to 7.5 ± 0.6 nM ($P < 0.01$). In a group with pretreatment of intravenous ANG II receptor subtype 1 (AT_1 receptor) blocker losartan (10 mg/kg, $n = 6$), ANG II was unable to inhibit the stimulation-induced ACh release (8.6 ± 1.5 vs. 8.4 ± 1.7 nM). In contrast, in a group with local administration of losartan (10 mM, $n = 6$) through the dialysis probe, ANG II inhibited the stimulation-induced ACh release (8.0 ± 0.8 vs. 5.8 ± 1.0 nM, $P < 0.05$). In conclusion, intravenous ANG II significantly inhibited the parasympathetic neurotransmission through AT_1 receptors. The failure of local losartan administration to nullify the inhibitory effect of ANG II on the stimulation-induced ACh release indicates that the site of this inhibitory action is likely at parasympathetic ganglia rather than at postganglionic vagal nerve terminals.

cardiac microdialysis; cats; losartan

ANG II HAS a variety of effects on the cardiovascular system (22): it acts on the vascular beds to increase peripheral vascular resistance and also on the adrenal cortex to cause volume retention. These direct effects of ANG II contribute to the maintenance of arterial pressure (AP). Aside from these direct effects, ANG II has been shown to modulate the sympathetic nervous system both centrally (7, 9) and peripherally (10). With respect to the sympathetic regulation in the heart, however, exogenous ANG II does not facilitate stimulation- and ischemia-induced norepinephrine release in the porcine left ventricle (18). Compared with a number of reports on the sympathetic system, only a few reports are available as to the effects of ANG II on the parasympathetic system. In 1982, Potter (23) demonstrated that ANG II (5–10 μg iv, body wt not reported) inhibited bradycardia induced by vagal stimulation in dogs. In that study, administration of ACh reduced the heart rate to an identical degree in the presence or absence of ANG II, suggesting that the inhibition of bradycardia by ANG II was attributable to the inhibition of the ACh release from the vagal nerve terminals. In contrast, Andrews et al. (3) reported that ANG II (500 ng/kg iv) did not inhibit bradycardia induced by vagal stimulation in ferrets. In a rat heart failure model, ANG II receptor subtype 1 (AT_1 receptor) antagonist losartan enhanced the bradycardic response to vagal stimulation (5). In pithed rats, an angiotensin-converting enzyme (ACE) inhibitor captopril also enhanced the bradycardic response to vagal stimulation (25, 26). In all of these studies, changes in the heart rate were used as a functional measurement of peripheral vagal function because of the difficulty in measuring the ACh release in the in vivo heart. Accordingly, whether ANG II affects the vagal control over the ventricle remains unknown. The aim of the present study was to examine the effect of ANG II on the vagal stimulation-induced ACh release in the left ventricular myocardium by measuring the interstitial ACh levels directly using a cardiac microdialysis technique (1, 13–15). We also explored the possible sites of action for the effect of ANG II on the stimulation-induced ACh release by administering losartan systemically from the femoral vein or locally through the dialysis fiber. Because ACh has a protective effect on the ischemic myocardium (12, 24, 29), elucidating the effect of ANG II on the ACh release in the ventricle would be helpful to understand the mechanism of ACE inhibitor or AT_1 receptor antagonist for the treatment of heart diseases (16, 17).

MATERIALS AND METHODS

Surgical Preparation

Animal care was provided in strict accordance with the *Guiding Principles for the Care and Use of Animals in the Field of Physiological Sciences* approved by the Physiological Society of Japan. All protocols were approved by the Animal Subject Committee of the National Cardiovascular Center. Twenty eight adult cats weighing from 1.9 to 4.9 kg were anesthetized using an intraperitoneal injection of pentobarbital sodium (30–35 mg/kg) and were then ventilated mechanically with room air mixed with oxygen. The depth of anesthesia was maintained by a continuous intravenous infusion of pentobarbital sodium (1–2 $mg \cdot kg^{-1} \cdot h^{-1}$) through a catheter inserted in the right femoral vein. Systemic AP was monitored by a catheter inserted in the right femoral artery. Heart rate was determined from an

Address for reprint requests and other correspondence: T. Kawada, Dept. of Cardiovascular Dynamics, National Cardiovascular Center Research Institute, 5-7-1 Fujishirodai, Suita, Osaka 565-8565, Japan (e-mail: torukawa@res.ncvc.go.jp).

The costs of publication of this article were defrayed in part by the payment of page charges. The article must therefore be hereby marked "*advertisement*" in accordance with 18 U.S.C. Section 1734 solely to indicate this fact.

electrocardiogram using a cardiotachometer. Esophageal temperature of the animal, measured using a thermometer (CTM-303; TERUMO), was maintained at ~37°C using a heating pad and a lamp. Both vagal nerves were exposed and sectioned bilaterally through a midline cervical incision. With the animal in the lateral position, we resected the left fifth and sixth ribs to approach the heart. After the incision of the pericardium, the heart was suspended in a pericardial cradle. Stainless steel wires were attached to the apex and the posterior wall of the left ventricle to pace the heart. Using a fine guiding needle, we implanted a dialysis probe transversely through the anterolateral free wall of the left ventricle. Next, we attached a pair of bipolar platinum electrodes to the cardiac end of each sectioned vagal nerve. The nerves and electrodes were covered in warmed mineral oil for insulation. We gave heparin sodium (100 U/kg) intravenously to prevent blood coagulation. At the end of the experiment, postmortem examination confirmed that the semipermeable membrane of the dialysis probe had been implanted in the left ventricular myocardium.

Dialysis Technique

The materials and properties of the dialysis probe have been described previously (1). Briefly, we designed a transverse dialysis probe in which a dialysis fiber of semipermeable membrane (13 mm length, 310 μm outer diameter, 200 μm inner diameter; PAN-1200, 50,000 mol wt cutoff; Asahi Chemical) was attached at both ends to polyethylene tubes (25 cm length, 500 μm outer diameter, 200 μm inner diameter). The dialysis probe was perfused at a rate of 2 μl/min with Ringer solution containing the cholinesterase inhibitor physostigmine (100 μM). Experimental protocols were started 2 h after implanting the dialysis probe when the ACh concentration in the dialysate reached a steady state. ACh concentrations in the dialysate were measured by an HPLC system with electrochemical detection (Eicom, Kyoto, Japan).

Figure 1 schematizes the three original protocols and two supplemental protocols utilized in the present study. The hatched rectangle indicates the baseline sampling, whereas the solid rectangles indicate the sampling during the 10-min vagal stimulation period (1 ms, 10 V, 20 Hz) in each protocol. The stimulus was set supramaximal to most easily delineate the possible effect of ANG II on myocardial interstitial ACh release. In all of the vagal stimulation periods, we paced the heart at 200 beats/min to avoid the difference in heart rate affecting the vagal stimulation-induced ACh release (14). For baseline sampling periods, we paced the heart at 200 beats/min when spontaneous heart rate was <200 beats/min.

Protocol 1 (n = 6). We examined the effects of intravenous administration of ANG II on vagal stimulation-induced myocardial ACh release. We collected a dialysate sample under baseline conditions. We then stimulated the vagal nerve and paced the heart for 10 min and collected a dialysate sample during the stimulation period

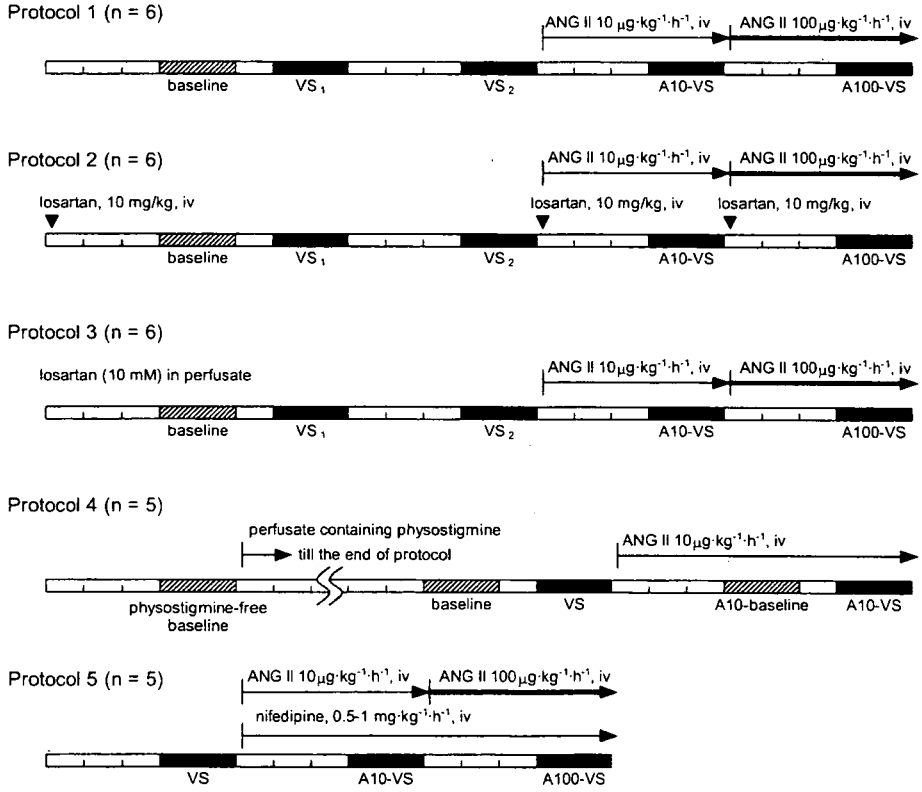

Fig. 1. Schematic representation of the protocols used in the present study. After implantation of the dialysis probe (2 h), we obtained a baseline dialysate sample (hatched rectangles) for 10 min. Thereafter, we obtained 4 dialysate samples during vagal stimulation with fixed-rate pacing for 10 min (filled rectangles) at intervening intervals of 15 min. In *protocols 1* through *3*, after obtaining 2 control trials (VS_1 and VS_2), we initiated intravenous administration of ANG II at 10 $\mu g \cdot kg^{-1} \cdot h^{-1}$ and waited for 15 min to obtain a dialysate sample during vagal stimulation with fixed-rate pacing (A10-VS). We then increased the dose of ANG II to 100 $\mu g \cdot kg^{-1} \cdot h^{-1}$ and waited for an additional 15 min before obtaining a dialysate sample during vagal stimulation with fixed-rate pacing (A100-VS). In *protocol 2*, the ANG II receptor subtype 1 blocker losartan was administered by bolus injection (10 mg/kg) before obtaining a baseline dialysate sample and also immediately before the beginning of each dose of ANG II administration (▼). In *protocol 3*, we administered losartan (10 mM) through the dialysis probe throughout the protocol. In *protocol 4*, we first collected a dialysate sample using perfusate free of physostigmine. We then replaced the perfusate with Ringer solution containing physostigmine and collected dialysate samples of baseline and vagal stimulation (VS). Approximately 15 min after the onset of iv ANG II administration at 10 $\mu g \cdot kg^{-1} \cdot h^{-1}$, we collected dialysate samples of baseline (A10-baseline) and vagal stimulation (A10-VS). In *protocol 5*, we collected dialysate samples during a control vagal stimulation (VS) and during the 2 doses of iv ANG II administration (A10-VS and A100-VS). The pressor effect of ANG II was counteracted by simultaneous iv infusion of the L-type Ca^{2+} channel blocker nifedipine.

(VS_1). After an intervening interval of 15 min, we repeated the 10-min vagal stimulation with fixed-rate pacing and collected another dialysate sample (VS_2). After performing these two control trials, we began intravenous administration of ANG II at 10 $\mu g \cdot kg^{-1} \cdot h^{-1}$. Approximately 15 min after the onset of the ANG II administration, we collected a dialysate sample (A10-VS) during 10-min vagal stimulation with fixed-rate pacing. We then increased the dose of ANG II at 100 $\mu g \cdot kg^{-1} \cdot h^{-1}$. Approximately 15 min after the onset of the higher-dose ANG II administration, we collected a final dialysate sample (A100-VS) during 10-min vagal stimulation with fixed-rate pacing.

Protocol 2 (n = 6). We examined whether the intravenous AT_1 receptor antagonist losartan would block the effects of ANG II on the vagal stimulation-induced myocardial ACh release. We infused losartan potassium intravenously at 10 mg/kg and waited for ~15 min. We then collected baseline, VS_1, and VS_2 samples with an intervening interval of 15 min, as described in *protocol 1*. Next, after an additional bolus injection of losartan potassium at 10 mg/kg, we began intravenous infusion of ANG II at 10 $\mu g \cdot kg^{-1} \cdot h^{-1}$. After ~15 min, we obtained a dialysate sample of A10-VS. Finally, after another bolus injection of losartan potassium at 10 mg/kg, we began intravenous infusion of ANG II at 100 $\mu g \cdot kg^{-1} \cdot h^{-1}$. After an additional 15 min, we obtained a dialysate sample of A100-VS.

Protocol 3 (n = 6). We examined whether local administration of losartan would block the effects of ANG II on the vagal stimulation-induced myocardial ACh release. We perfused the dialysis probe with Ringer solution containing 10 mM of losartan potassium. Taking into account the distribution across the semipermeable membrane, we administered losartan at a concentration >400 times higher than that for intravenous administration in *protocol 2*. Because local administrations of larger molecules such as ω-conotoxin GVIA (molecular weight 3037) and ω-conotoxin MVIIC (mol wt 2,749) were able to suppress vagal stimulation-induced ACh release in our previous study (15), it would be reasonable to assume that losartan potassium (mol wt 461) should have spread in the vicinity of the dialysis fiber, from which the dialysate was collected. Using the same procedures as described in *protocol 1*, we obtained dialysate samples for baseline, VS_1, VS_2, A10-VS, and A100-VS. A previous study indicated that ACh measured by cardiac microdialysis in the left ventricle mainly reflected ACh released from the postganglionic nerve terminals and not from the parasympathetic ganglia (1 and see DISCUSSION for details).

Protocol 4 (n = 5). To examine the effects of ANG II on the baseline ACh level, we performed an additional protocol where the baseline ACh level was measured during intravenous infusion of ANG II at 10 $\mu g \cdot kg^{-1} \cdot h^{-1}$ (A10-baseline). In this protocol, we also obtained a dialysate sample using the perfusate without the cholinesterase inhibitor physostigmine before the usual dialysate sampling using the perfusate containing physostigmine.

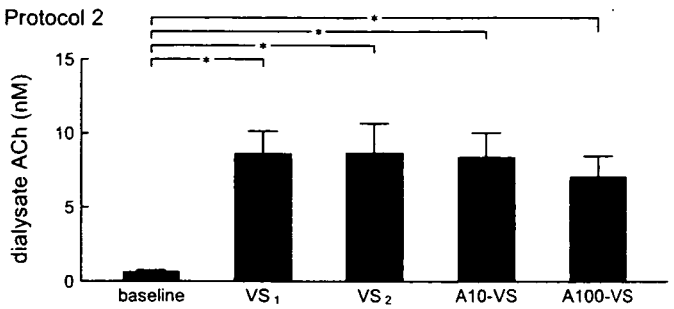

Fig. 3. Changes in dialysate ACh concentrations obtained from *protocol 2*. Vagal stimulation significantly increased the ACh levels. There was no significant difference in the ACh level among the 4 dialysate samples during vagal stimulation (VS_1, VS_2, A10-VS, and A100-VS). Values are presented as means and SE. $*P < 0.01$ by Tukey's test.

Protocol 5 (n = 5). To avoid the pressor effect of ANG II, we administered an L-type Ca^{2+} channel blocker nifedipine (0.5–2.0 $mg \cdot kg^{-1} \cdot h^{-1}$) simultaneously with ANG II and obtained dialysate samples for VS, A10-VS, and A100-VS. In a previous study, intravenous administration of an L-type Ca^{2+} channel blocker alone did not affect the vagal stimulation-induced myocardial ACh release significantly (15).

Statistical Analysis

All data are presented as mean ± SE values. In *protocols 1* through *3*, myocardial interstitial ACh levels were compared among baseline, VS_1, VS_2, A10-VS, and A100-VS samples using a repeated-measures ANOVA (8). When there was a significant difference, Tukey's test for all-pairwise comparisons was applied to identify the differences between any two of the samples. Differences were considered significant at $P < 0.05$. The mean AP value in the last 1 min of the 10-min vagal stimulation period was treated as the AP value during vagal stimulation. The AP data were compared using a repeated-measures ANOVA among baseline, during the two control stimulations (VS_1 and VS_2), and before and during vagal stimulation under the two different doses of intravenous ANG II administrations. When there was a significant difference, Dunnett's test for comparison against a single control was applied to identify differences from the baseline value. Differences were considered significant at $P < 0.05$. In

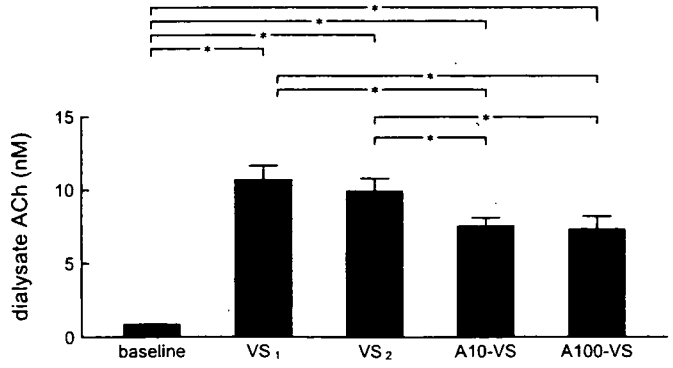

Fig. 2. Changes in dialysate ACh concentrations obtained from *protocol 1*. Vagal stimulation significantly increased the ACh levels. There was no significant difference in the ACh level between the 2 control trials (VS_1 and VS_2). The ACh level was significantly lower in A10-VS and A100-VS compared with that measured in VS_1 and VS_2. There was no significant difference in the ACh level between A10-VS and A100-VS. Values are presented as mean and SE. $*P < 0.01$ by Tukey's test.

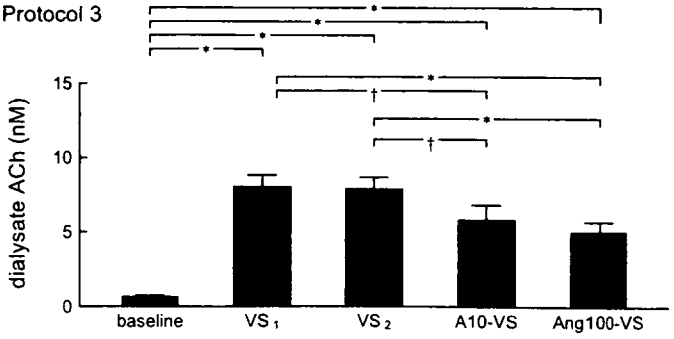

Fig. 4. Changes in dialysate ACh concentrations obtained from *protocol 3*. Vagal stimulation significantly increased the ACh levels. There was no significant difference in the ACh level between the 2 control trials (VS_1 and VS_2). The ACh level was significantly lower in A10-VS and A100-VS compared with that measured in VS_1 and VS_2. There was no significant difference in the ACh level between A10-VS and A100-VS. Values are presented as means and SE. $\dagger P < 0.05$ and $*P < 0.01$ by Tukey's test.

Table 1. *Mean arterial pressure values before vagal stimulation and during the last 1 min of stimulation*

	Baseline	VS_1	VS_2	A10	A10-VS	A100	A100-VS
Protocol 1	102±11	93±17	91±17	132±9†	105±19	129±13†	105±21
Protocol 2	102±17	71±16*	69±16*	80±15	68±17*	86±19	72±18*
Protocol 3	102±13	100±17	92±17	139±11*	120±19	147±11*	122±21

Data are means ± SE obtained from baseline, two control trials (VS_1 and VS_2), before (A10) and during (A10-VS) vagal stimulation under iv administration of ANG II at 10 $\mu g \cdot kg^{-1} \cdot h^{-1}$, and before (A100) and during (A100-VS) vagal stimulation under iv administration of ANG II at 100 $\mu g \cdot kg^{-1} \cdot h^{-1}$. The heart was paced at 200 beats/min whenever vagal stimulation was applied. †$P < 0.05$ and *$P < 0.01$ from the respective baseline values by Dunnett's test.

protocol 4, the baseline ACh levels were compared before and during the ANG II administration using a paired *t*-test. The ACh levels during vagal stimulation were also compared before and during ANG II administration using a paired *t*-test. In *protocol 5*, the ACh levels and the mean AP values were compared among VS, A10-VS, and A100-VS using a repeated-measures ANOVA followed by Tukey's test.

RESULTS

In *protocol 1*, vagal stimulation significantly increased myocardial interstitial ACh levels (Fig. 2). There was no significant difference between two control trials with an intervening interval of 15 min [VS_1: 10.7 ± 1.0 (SE) nM and VS_2: 9.9 ± 0.9 (SE) nM]. Intravenous administration of ANG II at 10 $\mu g \cdot kg^{-1} \cdot h^{-1}$ significantly attenuated the vagal stimulation-induced ACh release (A10-VS: 7.5 ± 0.6 nM) to ~71% of VS_1. Although the intravenous administration of ANG II at 100 $\mu g \cdot kg^{-1} \cdot h^{-1}$ also significantly attenuated the vagal stimulation-induced ACh release (A100-VS: 7.3 ± 0.9 nM) to ~68% of VS_1, the ACh levels were not different from those of A10-VS.

In *protocol 2*, vagal stimulation significantly increased myocardial interstitial ACh levels under control stimulations (VS_1: 8.6 ± 1.5 nM and VS_2: 8.7 ± 2.0 nM; Fig. 3). With a pretreatment of intravenous losartan, intravenous ANG II was unable to suppress the vagal stimulation-induced ACh release (A10-VS: 8.4 ± 1.7 nM and A100-VS: 7.1 ± 1.4 nM). Although the mean level of ACh tended to be lower in A100-VS compared with VS_1 or VS_2, the differences were not statistically significant.

In *protocol 3*, vagal stimulation significantly increased myocardial interstitial ACh levels under control stimulations (VS_1: 8.0 ± 0.8 nM and VS_2: 7.9 ± 0.8 nM; Fig. 4). Intravenous ANG II at either 10 $\mu g \cdot kg^{-1} \cdot h^{-1}$ or 100 $\mu g \cdot kg^{-1} \cdot h^{-1}$ significantly suppressed the vagal stimulation-induced ACh release to ~72% (A10-VS: 5.8 ± 1.0 nM) and 62% (A100-VS: 5.0 ± 0.7 nM of that seen in VS_1), respectively.

In *protocol 1*, the AP values before the vagal stimulation during the intravenous ANG II administrations (A10 and A100) were significantly higher than the baseline AP value (Table 1). The AP values during vagal stimulation (VS_1, VS_2, A10-VS, and A100-VS) were not different from the baseline AP value. In *protocol 2*, the AP value before the first administration of losartan was 126 ± 14 mmHg. The AP values before the vagal stimulation during the intravenous ANG II administrations (A10 and A100) were not significantly different from the baseline AP value. The AP values during vagal stimulation (VS_1, VS_2, A10-VS, and A100-VS) were significantly lower than the baseline AP value. In *protocol 3*, the AP values before vagal stimulation during the intravenous ANG II administrations (A10 and A100) were significantly higher than the baseline AP value. The AP values during vagal stimulation (VS_1, VS_2, A10-VS, and A100-VS) did not differ statistically from the baseline AP value.

Figure 5 illustrates typical chromatograms obtained from one animal in *protocol 4*. The baseline ACh level was below the limit of determination (0.5 nM) when the perfusate did not contain physostigmine. Approximately 1 h after replacing the perfusate with Ringer solution containing physostigmine, the baseline ACh level was above the limit of determination. As shown in Table 2, vagal stimulation significantly increased the ACh level (VS). The intravenous administration of ANG II did not affect the baseline ACh level (A10-basline) but significantly attenuated the ACh level during vagal stimulation (A10-VS).

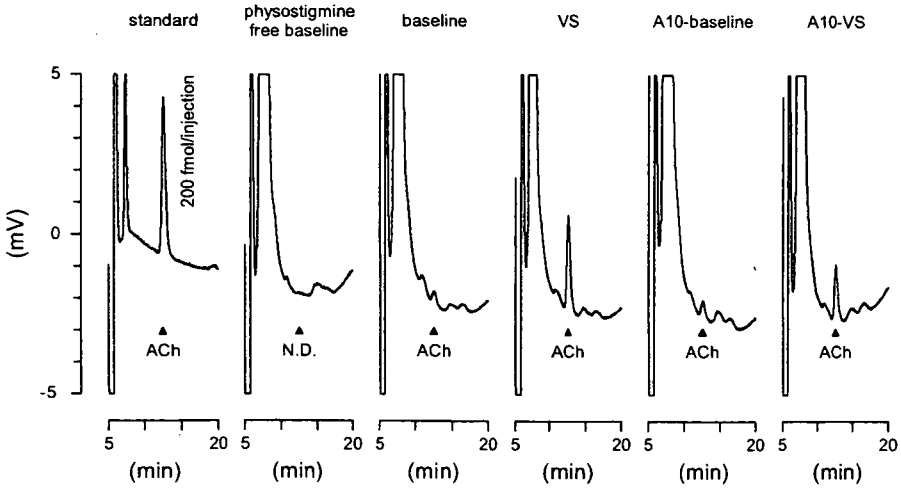

Fig. 5. Typical chromatograms for the ACh measurements obtained from *protocol 4*. ACh was less than the limit of determination when perfusate did not contain physostigmine (physostigmine-free baseline). The baseline ACh level was above the limit of determination when perfusate contained 100 μM physostigmine. (This perfusate was usually used for the ACh measurements.) Vagal stimulation increased the ACh level (VS). The administration of ANG II at 10 $\mu g \cdot kg^{-1} \cdot h^{-1}$ did not affect baseline ACh level (A10-baseline) but significantly attenuated the vagal stimulation-induced ACh release (A10-VS). See Table 2 for pooled data of ACh levels. ND, not detected.

Table 2. *Mean arterial pressure values and ACh concentrations obtained in protocol 4*

	Physostigmine-free Baseline	Baseline	VS	A10-Baseline	A10-VS
ACh, nM	Not detected	1.6±0.4	10.6±2.4	1.7±0.5	7.8±2.1*
Mean arterial pressure, mmHg	111±11	109±12	103±6	148±3*	118±6

Data are means ± SE obtained from physostigmine-free baseline, baseline, control vagal stimulation (VS), and baseline (A10-baseline) and vagal stimulation (A10-VS) under iv administration of ANG II at 10 $\mu g \cdot kg^{-1} \cdot h^{-1}$. There was no significant difference in the ACh level between baseline and A10-baseline by a paired-*t*-test. The ACh level was significantly lower in A10-VS than in VS by a paired-*t*-test. Mean arterial pressure was significantly higher in A10-baseline compared with the physostigmine-free baseline value by Dunnett's test. *$P < 0.01$.

In *protocol 5*, the pressor effect of ANG II was counteracted by the simultaneous intravenous infusion of nifedipine (Table 3). Under this condition, the intravenous administration of ANG II significantly attenuated the stimulation-induced ACh level to ~83% (A10-VS) and 72% (A100-VS) of that seen in VS.

DISCUSSION

The present study demonstrated that intravenous ANG II significantly inhibited the vagal stimulation-induced myocardial interstitial ACh release in the left ventricle in anesthetized cats. Intravenous administration of losartan abolished the inhibitory effect of ANG II on the stimulation-induced ACh release, suggesting that the inhibitory action of ANG II was mediated by AT_1 receptors.

Inhibitory Effect of ANG II on Myocardial Interstitial ACh Release

Only a few reports have focused on the modulatory effects of ANG II on the parasympathetic nervous system (3, 5, 25, 26), all of which have used the heart rate reduction in response to vagal stimulation as a functional measurement to assess the peripheral vagal function. Although ANG II has been shown to inhibit the ACh release in the rat entorhinal cortex in vitro (4), the direct evidence for the inhibitory effect of ANG II on the ACh release in the peripheral vagal neurotransmission in vivo has been lacking. The present study demonstrated that intravenous ANG II inhibited the vagal nerve stimulation-induced ACh release in the left ventricle in vivo (Fig. 2). As for the sympathetic system in the heart, Lameris et al. (18) have previously demonstrated that ANG II does not affect the sympathetic nerve stimulation-induced norepinephrine release. The insignificant effect of ANG II on the sympathetic neurotransmission and the inhibitory effect of ANG II on the parasympathetic neurotransmission may provide the basis for a study by Takata et al. (26) in which ACE inhibitor enhanced cardiac vagal but not sympathetic neurotransmission.

Table 3. *Mean arterial pressure values and ACh concentrations obtained in protocol 5*

	VS	A10-VS	A100-VS
ACh, nM	12.7±1.1	10.6±1.1†	9.2±1.5*
Mean arterial pressure, mmHg	83.4±12.2	68.4±6.3	70.4±9.5

Data are means ± SE from a control vagal stimulation trial (VS), during vagal stimulation under iv administration of ANG II at 10 $\mu g \cdot kg^{-1} \cdot h^{-1}$ (A10-VS) and during vagal stimulation under iv administration of ANG II at 100 $\mu g \cdot kg^{-1} \cdot h^{-1}$ (A100-VS). The heart was paced at 200 beats/min during vagal stimulation. In this protocol, the pressor effect of ANG II was counteracted by simultaneous iv administration of the L-type Ca^{2+} channel blocker nifedipine (0.5–2 $mg \cdot kg^{-1} \cdot h^{-1}$). †$P < 0.05$ and *$P < 0.01$ from the VS group by Tukey's test. There was no significant difference between A10-VS and A100-VS in the ACh level. There were no significant differences in mean arterial pressure among the three trials.

An increased activity of the renin-angiotensin system is common in chronic heart failure and has been considered to be a stimulus for aggravation of the disease. Inhibition of the renin-angiotensin system by ACE inhibitors or by AT_1 receptor blockers can prevent the ventricular remodeling and improve the survival rate (16, 17), suggesting that ANG II is indeed involved in the aggravation of heart failure. ACh, on the other hand, can exert a cardioprotective effect against myocardial ischemia in several experimental settings (12, 24, 29). If ANG II inhibits the peripheral vagal neurotransmission, blockade of ANG II would increase the vagal effect on the heart. Actually, Du et al. (5) demonstrated that losartan enhanced bradycardia induced by vagal stimulation in rats with chronic myocardial infarction. In that study, however, the ventricular effect of vagal stimulation was not assessed. The results of the present study indicate that ANG II inhibited the vagal neurotransmission in the ventricle. Blockade of ANG II is therefore expected to increase the vagal effect on the ventricular myocardium when the vagal outflow from the central nervous system is unchanged. Although no literatures appear to be available as to the chronic effect of ACh on the prognosis of heart failure, electrical vagal stimulation was able to improve the survival rate of chronic heart failure in rats (19). In that study, the magnitude of the vagal stimulation was such that the heart rate decreased only by 20–30 beats/min in rats, suggesting that a modest increase in vagal tone would be sufficient to produce a cardioprotective effect. It is plausible that blockade of ANG II yields beneficial effects on chronic heart failure not only by antagonizing the sympathetic effects but also by enhancing the vagal effects on the ventricle.

Vagal stimulation was able to reduce the left ventricular contractility as assessed by end-systolic elastance only when sympathetic stimulation coexisted (20), suggesting that the effect of vagal stimulation on ventricular contractility would be secondary to sympathoinhibition. Accordingly, contribution of the inhibitory effect of ANG II on the stimulation-induced ACh release to the physiological regulation of ventricular contractility might be marginal. We think that the finding is important as a peripheral mechanism of vagal withdrawal in heart diseases accompanying the activation of the renin-angiotensin system.

Possible Site of the Inhibitory Action of ANG II on ACh Release

In *protocol 3*, we examined whether local administration of losartan was able to nullify the inhibitory effect of ANG II on the vagal stimulation-induced ACh release. The utility of local administration of pharmacological agents through the dialysis fiber has been confirmed previously. As an example, local administration the Na^+ channel inhibitor tetrodotoxin through the dialysis fiber completely blocked the nerve stimulation-induced ACh release (14). With respect to the source for ACh, intravenous administration of the nicotinic antagonist hexamethonium bromide completely blocked the stimulation-induced ACh release, whereas local administration of hexamethonium bromide did not, suggesting the lack of parasympathetic ganglia in the vicinity of dialysis fiber (1). In support of our interpretation, a neuroanatomic finding indicates that three ganglia, away from the left anterior free wall targeted by the dialysis probe, provide the major source of left ventricular postganglionic innervation in cats (11). Therefore, the myocardial interstitial ACh measured by cardiac microdialysis in the left ventricle mainly reflects the ACh release from the postganglionic vagal nerve terminals. The results of *protocol 3* indicate that losartan spread around the postganglionic vagal nerve terminals failed to abolish the inhibitory effect of ANG II on the stimulation-induced ACh release. Because intravenous administration of losartan was able to abolish the inhibitory effect of ANG II on the stimulation-induced ACh release (*protocol 2*), the site of this inhibitory action is likely at parasympathetic ganglia rather than at postganglionic vagal nerve terminals. The fact that AT_1 receptors are rich in parasympathetic ganglia (2) would support our interpretation.

ANG II has a direct vasoconstrictive effect on the coronary artery (30). At the same time, however, the intravenous administration of ANG II tended to increase mean AP during vagal stimulation by ~15 mmHg in *protocol 1* (Table 1). Although it was statistically insignificant, if this increase in mean AP increased cardiac oxygen demand, the coronary blood flow might have been increased (27), resulting in an increased rate of washout in the myocardial tissue. The possibility cannot be ruled out that such a washout mechanism contributed to the reduction of stimulation-induced ACh release during ANG II administration. However, the baseline ACh level was not decreased by ANG II in *protocol 4*, suggesting that the washout rate did not increase significantly. In addition, even when the pressor effect of ANG II was counteracted by nifedipine, ANG II was still able to inhibit the vagal stimulation-induced ACh release in *protocol 5*. Therefore, we think that the change in washout rate was not a principal mechanism for the reduction of stimulation-induced ACh release by ANG II.

The mechanisms for the baseline ACh release under the vagotomized condition were not identified in the present study. In the motor nerve terminals, a so-called nonquantal release of ACh is documented, which is independent of nerve activity (6). Incorporation of the vesicular transport system in the membrane of the nerve terminals during an exocytosis process is considered to be responsible for the mechanism of nonquantal ACh release. A similar mechanism might contribute to the baseline ACh release in the vagal nerve terminals.

Several limitations need to be addressed. First, the dose of ANG II might have increased the plasma ANG II concentration beyond the physiological range. In this regard, the observed effect might be rather pharmacological or pathological than physiological. Nevertheless, because there are local synthesis and degradation of ANG II in the heart (21, 28), the inhibition of ACh release by ANG II could operate locally in the heart. Second, whether ANG II inhibited the ACh release from the preganglionic nerve terminals or it suppressed the excitability of the postganglionic nerve fibers to ACh was not identified in the present study. Third, the involvement of ANG II receptor subtype 2 (AT_2 receptor) in the modulation of peripheral parasympathetic neurotransmission was not examined in the present study because intravenous losartan was able to abolish the inhibitory effect of ANG II on the stimulation-induced ACh release. However, if coactivation of AT_1 and AT_2 receptors is required for the inhibitory effect of ANG II, blockade of AT_2 receptors would also abolish the inhibitory effect. Forth, we tested just one level of vagal stimulation. Whether the effect of ANG II on the stimulation-induced ACh release depends on the vagal stimulation intensity remains to be resolved.

In conclusion, intravenous ANG II reduced the vagal nerve stimulation-induced ACh release in the left ventricle. Intravenous losartan abolished the inhibitory effect of ANG II on the stimulation-induced ACh release, suggesting that this inhibition was mediated by AT_1 receptors. Because local administration of losartan via dialysis fiber was unable to nullify the inhibitory effect of ANG II on the stimulation-induced ACh release, the site of this inhibitory action is likely parasympathetic ganglia. The present results imply that the beneficial effects of ACE inhibitors and AT_1 receptor antagonists in the treatment of heart diseases may include not only the suppression of sympathetic activity but also the enhancement of vagal activity to the ventricle.

GRANTS

This study was supported by a Health and Labour Sciences Research Grant for Research on Advanced Medical Technology, a Health and Labour Sciences Research Grant for Research on Medical Devices for Analyzing, Supporting, and Substituting the Function of Human Body, and Health and Labour Sciences Research Grant H18-Iryo-Ippan-023 from the Ministry of Health, Labour, and Welfare of Japan.

REFERENCES

1. **Akiyama T, Yamazaki T, Ninomiya I.** In vivo detection of endogenous acetylcholine release in cat ventricles. *Am J Physiol Heart Circ Physiol* 266: H854–H860, 1994.
2. **Allen AM, Zhuo J, Mendelsohn FA.** Localization and function of angiotensin AT_1 receptors. *Am J Hypertens* 13: 31S–38S, 2000.
3. **Andrews PL, Dutia MB, Harris PJ.** Angiotensin II does not inhibit vagally-induced bradycardia or gastric contractions in the anaesthetized ferret. *Br J Pharmacol* 82: 833–837, 1984.
4. **Barnes JM, Barnes NM, Costall B, Horovitz ZP, Naylor RJ.** Angiotensin II inhibits the release of [^{3}H]acetylcholine from rat entorhinal cortex in vitro. *Brain Res* 491: 136–143, 1989.
5. **Du XJ, Cox HS, Dart AM, Esler MD.** Depression of efferent parasympathetic control of heart rate in rats with myocardial infarction: effect of losartan. *J Cardiovasc Pharmacol* 31: 937–944, 1998.
6. **Edwards C, Doležal V, Tuček S, Zemková H, Vyskočil F.** Is an acetylcholine transport system responsible for nonquantal release of acetylcholine at the rodent myoneural junction? *Proc Natl Acad Sci USA* 82: 3354–3518, 1985.
7. **Gao L, Wang W, Li Y, Schultz HD, Liu D, Cornish KG, Zucker IH.** Sympathoexcitation by central ANG II: roles for AT_1 receptor upregulation and NAD(P)H oxidase in RVLM. *Am J Physiol Heart Circ Physiol* 288: H2271–H2279, 2005.
8. **Glantz SA.** *Primer of Biostatistics* (5th ed.). New York: McGraw-Hill, 2002.

9. **Hirooka Y, Head GA, Potts PD, Godwin SJ, Bendle RD, Dampney RA.** Medullary neurons activated by angiotensin II in the conscious rabbit. *Hypertension* 27: 287–296, 1996.
10. **Hughes J, Roth RH.** Evidence that angiotensin enhances transmitter release during sympathetic nerve stimulation. *Br J Pharmacol* 41: 239–255, 1971.
11. **Johnson TA, Gray AL, Lauenstein JM, Newton SS, Massari VJ.** Parasympathetic control of the heart. *I.* An interventriculo-septal ganglion is the major source of the vagal intracardiac innervation of the ventricles. *J Appl Physiol* 96: 2265–2272, 2004.
12. **Kakinuma Y, Ando M, Kuwabara M, Katare RG, Okudela K, Kobayashi M, Sato T.** Acetylcholine from vagal stimulation protects cardiomyocytes against ischemia and hypoxia involving additive non-hypoxic induction of HIF-1alpha. *FEBS Lett* 579: 2111–2118, 2005.
13. **Kawada T, Yamazaki T, Akiyama T, Sato T, Shishido T, Inagaki M, Takaki H, Sugimachi M, Sunagawa K.** Differential acetylcholine release mechanisms in the ischemic and non-ischemic myocardium. *J Mol Cell Cardiol* 32: 405–414, 2000.
14. **Kawada T, Yamazaki T, Akiyama T, Shishido T, Inagaki M, Uemura K, Miyamoto T, Sugimachi M, Takaki H, Sunagawa K.** In vivo assessment of acetylcholine-releasing function at cardiac vagal nerve terminals. *Am J Physiol Heart Circ Physiol* 281: H139–H145, 2001.
15. **Kawada T, Yamazaki T, Akiyama T, Uemura K, Kamiya A, Shishido T, Mori H, Sugimachi M.** Effects of Ca^{2+} channel antagonists on nerve stimulation-induced and ischemia-induced myocardial interstitial acetylcholine release in cats. *Am J Physiol Heart Circ Physiol* 291: H2187–H2191, 2006.
16. **Konstam MA, Neaton JD, Poole-Wilson PA, Pitt B, Segal R, Sharma D, Dasbach EJ, Carides GW, Dickstein K, Riegger G, Camm AJ, Martinez FA, Bradstreet DC, Ikeda LS, Santoro EP, investigators ELITEII.** Comparison of losartan and captopril on heart failure-related outcomes and symptoms from the losartan heart failure survival study (ELITE II). *Am Heart J* 150: 123–131, 2005.
17. **Konstam MA, Rousseau MF, Kronenberg MW, Udelson JE, Melin J, Stewart D, Dolan N, Edens TR, Ahn S, Kinan D, Howe DM, Kilcoyne L, Metherall J, Benedict C, Yusuf S, Pouleur H, investigators SOLVD.** Effects of the angiotensin converting enzyme inhibitor enalapril on the long-term progression of left ventricular dysfunction in patients with heart failure. *Circulation* 86: 431–438, 1992.
18. **Lameris TW, de Zeeuw S, Duncker DJ, Alberts G, Boomsma F, Verdouw PD, van den Meiracker AH.** Exogenous angiotensin II does not facilitate norepinephrine release in the heart. *Hypertension* 40: 491–497, 2002.
19. **Li M, Zheng C, Sato T, Kawada T, Sugimachi M, Sunagawa K.** Vagal nerve stimulation markedly improves long-term survival after chronic heart failure in rats. *Circulation* 109: 120–124, 2004.
20. **Nakayama Y, Miyano H, Shishido T, Inagaki M, Kawada T, Sugimachi M, Sunagawa K.** Heart rate-independent vagal effect on end-systolic elastance of the canine left ventricle under various levels of sympathetic tone. *Circulation* 104: 2277–2279, 2001.
21. **Paul M, Mehr AP, Kreutz R.** Physiology of local renin-angiotensin systems. *Physiol Rev* 86: 747–803, 2006.
22. **Peach MJ.** Renin-angiotensin system: Biochemistry and mechanisms of action. *Physiol Rev* 57: 313–370, 1977.
23. **Potter EK.** Angiotensin inhibits action of vagus nerve at the heart. *Br J Pharmacol* 75: 9–11, 1982.
24. **Qin Q, Downey JM, Cohen MV.** Acetylcholine but not adenosine triggers preconditioning through PI3-kinase and a tyrosine kinase. *Am J Physiol Heart Circ Physiol* 284: H727–H734, 2003.
25. **Rechtman M, Majewski H.** A facilitatory effect of anti-angiotensin drugs on vagal bradycardia in the pithed rat and guinea-pig. *Br J Pharmacol* 110: 289–296, 1993.
26. **Takata Y, Arai T, Suzuki S, Kurihara J, Uezono T, Okubo Y, Kato H.** Captopril enhances cardiac vagal but not sympathetic neurotransmission in pithed rats. *J Pharmacol Sci* 95: 390–393, 2004.
27. **Tune JD, Gorman MW, Feigl EO.** Matching coronary blood flow to myocardial oxygen consumption. *J Appl Physiol* 97: 404–415, 2004.
28. **van Kats JP, Danser AH, van Meegen JR, Sassen LM, Verdouw PD, Schalekamp MA.** Angiotensin production by the heart. A quantitative study in pigs with the use of radiolabeled angiotensin infusions. *Circulation* 98: 73–81, 1998.
29. **Yao Z, Gross GJ.** Acetylcholine mimics ischemic preconditioning via a glibenclamide-sensitive mechanism in dogs. *Am J Physiol Heart Circ Physiol* 264: H2221–H2225, 1993.
30. **Zhang C, Knudson JD, Setty S, Araiza A, Dincer üD, Kuo L, Tune JD.** Coronary arteriolar vasoconstriction to angiotensin II is augmented in prediabetic metabolic syndrome via activation of AT_1 receptors. *Am J Physiol Heart Circ Physiol* 288: H2154–H2162, 2005.

Am J Physiol Heart Circ Physiol 293: H1564–H1570, 2007.
First published May 25, 2007; doi:10.1152/ajpheart.00368.2007.

Muscarinic potassium channels augment dynamic and static heart rate responses to vagal stimulation

Masaki Mizuno,[1] Atsunori Kamiya,[1] Toru Kawada,[1] Tadayoshi Miyamoto,[1,2,3] Shuji Shimizu,[1,2] and Masaru Sugimachi[1]

[1]*Department of Cardiovascular Dynamics, Advanced Medical Engineering Center, National Cardiovascular Center Research Institute, and* [3]*Morinomiya University of Medical Sciences, Osaka; and* [2]*Japan Association for the Advancement of Medical Equipment, Tokyo, Japan*

Submitted 23 March 2007; accepted in final form 22 May 2007

Mizuno M, Kamiya A, Kawada T, Miyamoto T, Shimizu S, Sugimachi M. Muscarinic potassium channels augment dynamic and static heart rate responses to vagal stimulation. *Am J Physiol Heart Circ Physiol* 293: H1564–H1570, 2007. First published May 25, 2007; doi:10.1152/ajpheart.00368.2007.—Vagal control of heart rate (HR) is mediated by direct and indirect actions of ACh. Direct action of ACh activates the muscarinic K^+ (K_{ACh}) channels, whereas indirect action inhibits adenylyl cyclase. The role of the K_{ACh} channels in the overall picture of vagal HR control remains to be elucidated. We examined the role of the K_{ACh} channels in the transfer characteristics of the HR response to vagal stimulation. In nine anesthetized sinoaortic-denerved and vagotomized rabbits, the vagal nerve was stimulated with a binary white-noise signal (0–10 Hz) for examination of the dynamic characteristic and in a step-wise manner (5, 10, 15, and 20 Hz/min) for examination of the static characteristic. The dynamic transfer function from vagal stimulation to HR approximated a first-order, low-pass filter with a lag time. Tertiapin, a selective K_{ACh} channel blocker (30 nmol/kg iv), significantly decreased the dynamic gain from 5.0 ± 1.2 to 2.0 ± 0.6 (mean ± SD) beats·min^{-1}·Hz^{-1} ($P < 0.01$) and the corner frequency from 0.25 ± 0.03 to 0.06 ± 0.01 Hz ($P < 0.01$) without changing the lag time (0.37 ± 0.04 vs. 0.39 ± 0.05 s). Moreover, tertiapin significantly attenuated the vagal stimulation-induced HR decrease by 46 ± 21, 58 ± 18, 65 ± 15, and 68 ± 11% at stimulus frequencies of 5, 10, 15, and 20 Hz, respectively. We conclude that K_{ACh} channels contribute to a rapid HR change and to a larger decrease in the steady-state HR in response to more potent tonic vagal stimulation.

systems analysis; transfer function; muscarinic receptor; rabbit

VAGAL CONTROL OF HEART RATE (HR) is mediated by a cascade reaction to ACh release. ACh binds to M_2 muscarinic receptors and, consequently, decreases HR. However, the pathway is not simple; two different pathways mediate the ACh-induced HR decrease. The M_2 muscarinic receptors activate heterotrimeric G_i and/or G_o proteins in cardiac myocytes (18); the action of ACh is determined by the G_i protein subunits. Via a direct pathway, a G_i protein βγ-subunit activates inwardly rectifying muscarinic K^+ (K_{ACh}) channels in the sinoatrial node cells (11, 28, 35); K_{ACh} channels then exert a negative chronotropic effect by hyperpolarizing the sinoatrial node cells. On the other hand, via an indirect pathway, a G_i protein α-subunit suppresses adenylyl cyclase (12, 32); the suppression of adenylyl cyclase then decreases HR by inhibiting inward currents in the sinoatrial node cells, which are activated by cAMP or cAMP-dependent protein kinase. However, functional roles of the direct and indirect actions of ACh are not fully understood in the overall picture of vagal control of HR.

As a function in the dual control of adenylyl cyclase by G protein (12), the indirect action of ACh counteracts the G_s proteins activated by β_1-adrenergic sympathetic stimulation and relies on slower changes in intracellular cAMP levels (8). On the contrary, the direct action of ACh utilizes the faster membrane-delimited mechanisms involving K_{ACh} channels (3) and is believed to be independent of sympathetic control. Given the rapidity of vagal HR control compared with sympathetic control (2, 14, 31), we hypothesized that the direct action of ACh via K_{ACh} channels contributes to the quickness of the vagal HR control in vivo. To test this hypothesis, we used the selective K_{ACh} channel blocker tertiapin to examine the dynamic and static transfer characteristics of the HR response to vagal stimulation (7, 10, 13, 15).

The pioneering work by Yamada (34) demonstrated that the direct action of ACh via K_{ACh} channels mediates ~75% of the steady-state negative chronotropic effects relative to the maximum carbachol-induced bradycardia in the isolated rabbit heart (i.e., static HR response to vagal stimulation). However, in this study, the role of K_{ACh} channels in the dynamic HR response to vagal stimulation was not analyzed quantitatively. Because HR changes dynamically in response to daily activities, quantification of dynamic and static characteristics is equally important. For instance, information on the dynamic HR response is key to understanding the generation of HR variability. Berger et al. (2) used transfer function analysis to identify the dynamic characteristics of the HR response. Saul et al. (29) demonstrated the utility of transfer function analysis for insight into cardiovascular regulation. The present study aims to expand our knowledge of the involvement of K_{ACh} channels in dynamic HR control by the vagal system.

MATERIALS AND METHODS

Surgical preparations. Animal care was consistent with the "Guiding Principles for Care and Use of Animals in the Field of Physiological Sciences," of the Physiological Society of Japan. All protocols were reviewed and approved by the Animal Subjects Committee of the National Cardiovascular Center. Nine Japanese White rabbits (2.5–3.2 kg body wt) were anesthetized by a mixture of urethane (250 mg/ml) and α-chloralose (40 mg/ml): initiation with a bolus injection of 2 ml/kg and maintenance with continuous administration at 0.5

Address for reprint requests and other correspondence: M. Mizuno, Dept. of Cardiovascular Dynamics, Advanced Medical Engineering Center, National Cardiovascular Center Research Institute, 5-7-1 Fujishirodai, Suita, Osaka 565-8565, Japan (e-mail: m-mizuno@ri.ncvc.go.jp).

The costs of publication of this article were defrayed in part by the payment of page charges. The article must therefore be hereby marked "*advertisement*" in accordance with 18 U.S.C. Section 1734 solely to indicate this fact.

$ml \cdot kg^{-1} \cdot h^{-1}$. The rabbits were intubated and mechanically ventilated with oxygen-enriched room air. Arterial pressure (AP) was measured by a micromanometer (model SPC-330A, Millar Instruments, Houston, TX) inserted into the right femoral artery and advanced to the thoracic aorta. HR was measured with a cardiotachometer (model N4778, San-ei, Tokyo, Japan). A double-lumen catheter was introduced into the right femoral vein for continuous anesthetic and drug administration. Sinoaortic denervation was performed bilaterally to minimize changes in the sympathetic efferent nerve activity via arterial baroreflexes. Bilateral section of the cardiac postganglionic sympathetic nerves minimized any possible interaction between the vagus and sympathetic nerves. The vagi were sectioned bilaterally at the neck. A pair of bipolar electrodes were attached to the cardiac end of the sectioned right vagus for vagal stimulation. Immersion of the stimulation electrodes and nerves in a mixture of white petroleum jelly (Vaseline) and liquid paraffin prevented drying and provided insulation. Body temperature was maintained at 38°C with a heating pad throughout the experiment.

Experimental procedures. The pulse duration of nerve stimulation was set at 2 ms. The stimulation amplitude of the right vagus was adjusted to yield an HR decrease of ~50 beats/min at a stimulation frequency of 10 Hz. After this adjustment, the amplitude of vagal stimulation was fixed at 1.8–6.0 V. Initiation of vagal nerve stimulation over 1 h upon completion of surgical preparations allowed stable hemodynamics. A preliminary examination indicated that the response of HR to vagal stimulation was stable for up to 3 h in our experimental settings (10 min of dynamic vagal stimulation at 50-min intervals; data not shown).

Dynamic protocol. For estimation of the dynamic transfer characteristics from vagal stimulation to HR response, the right vagus was stimulated by a frequency-modulated pulse train for 10 min. The stimulation frequency was switched every 500 ms at 0 or 10 Hz according to a binary white-noise signal. The power spectrum of the stimulation signal was reasonably constant up to 1 Hz. The transfer function was estimated up to 1 Hz, because the reliability of estimation decreased as a result of the diminution of input power above this frequency. The selected frequency range sufficiently spanned the physiological range of interest with respect to the dynamic vagal control of HR.

Static protocol. For estimation of the static transfer characteristics from vagal stimulation to HR response, step-wise vagal stimulation was performed. Vagal stimulation frequency was increased from 5 to 20 Hz in 5-Hz increments. Each frequency step was maintained for 60 s.

The dynamic and static transfer functions from vagal stimulation to HR response were estimated under control and K_{ACh} channel blockade conditions. After the control data were recorded, a bolus injection (30 nmol/kg iv) of a selective K_{ACh} channel blocker, tertiapin (Peptide Institute, Osaka, Japan), was administered, and vagal stimulation protocols were repeated 15 min thereafter. The control data were obtained first in all animals, because the long-lasting (>2 h) effects of tertiapin (data not shown) did not permit the subsequent acquisition of control data. A >5-min interval between dynamic and step-wise stimulation protocols confirmed that AP and HR returned to baseline levels. Dynamic and step-wise vagal stimulation protocols were randomly assigned under control and K_{ACh} channel blockade conditions.

β-Adrenergic blockade protocol. A supplemental experiment was performed under β-adrenergic blockade ($n = 3$) eliminated any effect of sympathetic activity. At ~10 min after a bolus injection of propranolol (1 mg/kg iv) (22), HR and AP reached a new steady state. The dynamic and static transfer functions from vagal stimulation to HR response were estimated before and after tertiapin treatment, both under β-adrenergic blockade.

Data analysis. A 12-bit analog-to-digital converter was used to digitize data at 200 Hz, and data were stored on the hard disk of a dedicated laboratory computer system. The dynamic transfer function from binary white-noise vagal stimulation to HR response was estimated as follows. Input-output data pairs of the vagal stimulation frequency and HR were resampled at 10 Hz; then data pairs were partitioned into eight 50%-overlapping segments consisting of 1,024 data points each. For each segment, the linear trend was subtracted, and a Hanning window was applied. A fast Fourier transform was then performed to obtain the frequency spectra for vagal stimulation [N(f)] and HR [HR(f)] (4). Over the eight segments, the power of vagal stimulation [$S_{N \cdot N}(f)$], the power of HR [$S_{HR \cdot HR}(f)$], and the cross power between these two signals [$S_{N \cdot HR}(f)$] were ensemble averaged. Finally, the transfer function [$H(f)$] from vagal stimulation to the HR response was determined as follows (1, 20)

$$H(f) = \frac{S_{N \cdot HR}(f)}{S_{N \cdot N}(f)} \quad (1)$$

The transfer function from vagal stimulation to HR response approximated a first-order, low-pass filter with a lag time in previous studies (14, 21–24); therefore, the estimated transfer function was parameterized as follows

$$H(f) = \frac{-K}{1 + \frac{f}{f_C} j} e^{-2\pi f j L} \quad (2)$$

where K represents the dynamic gain (or, more precisely, the steady-state gain, in beats·min^{-1}·Hz^{-1}), f_c denotes the corner frequency (in Hz), L denotes the lag time (in s), and f and j represent frequency and the imaginary unit, respectively. The negative sign in the numerator indicates the negative HR response to vagal stimulation. The steady-state gain indicates the asymptotic value of the relative amplitude of the HR response to vagal nerve stimulation obtained in the frequency of input modulation approaching zero. The corner frequency represents the frequency of input modulation at which gain decreases by 3 dB from the steady-state gain in the frequency domain and reflects the readiness of the HR response for vagal stimulation in the time domain. The dynamic gain, corner frequency, and lag time were estimated by an iterative nonlinear least-squares regression. The phase shift of the transfer function indicates, with respect to the input signal, a lag or lead in the output signal normalized by its corresponding frequency of input modulation.

To quantify the linear dependence of the HR response on vagal stimulation, the magnitude-squared coherence function [Coh(f)] was estimated as follows (1, 20)

$$\mathrm{Coh}(f) = \frac{|S_{N \cdot HR}(f)|^2}{S_{N \cdot N}(f) \cdot S_{HR \cdot HR}(f)} \quad (3)$$

Coherence values range from zero to unity. Unity coherence indicates perfect linear dependence between the input and output signals; in contrast, zero coherence indicates total independence between the two signals.

To facilitate the intuitive understanding of the system dynamic characteristics, we calculated the system step response of HR to 1-Hz nerve stimulation as follows. The system impulse response was derived from the inverse Fourier transform of $H(f)$. The system step response was then obtained from the time integral of the impulse response. The length of the step response was 51.2 s. We calculated the maximum step response by averaging the last 10 s of the step response. The 90% rise time of the step response was determined as the time required for the response to reach 90% of the maximum step response. The time constant of the step response was calculated from the corner frequency of the corresponding transfer function as follows

$$\text{time constant} = \frac{1}{2 \cdot \pi \cdot fc} \quad (4)$$

where the time constant is related inversely to the corner frequency without influence of the lag time.

The static transfer function from step-wise vagal stimulation to HR was estimated by averaging the HR data during the final 10 s of the 60-s stimulation at each stimulation frequency.

Statistical analysis. Values are means ± SD. Student's paired *t*-test was used to test differences in fitted parameters and calculated step response between control and K_{ACh} channel blockade conditions. For hemodynamic parameters, a two-way ANOVA, with drug and vagal stimulation as the main effects, was used to determine significant differences. For percent reduction from the control conditions in each parameter, one-way ANOVA was used to determine significant differences. $P < 0.05$ was considered significant.

RESULTS

Dynamic characteristics. Figure 1*A* shows typical recordings and corresponding power spectra of vagal stimulation and HR response under control and K_{ACh} channel blockade conditions. Random vagal stimulation decreased HR intermittently. Tertiapin-mediated K_{ACh} channel blockade attenuated the amplitude of the variation and the speed of the HR response to vagal stimulation. In the power spectral plot, tertiapin decreased the HR power. The decrease in the HR power was

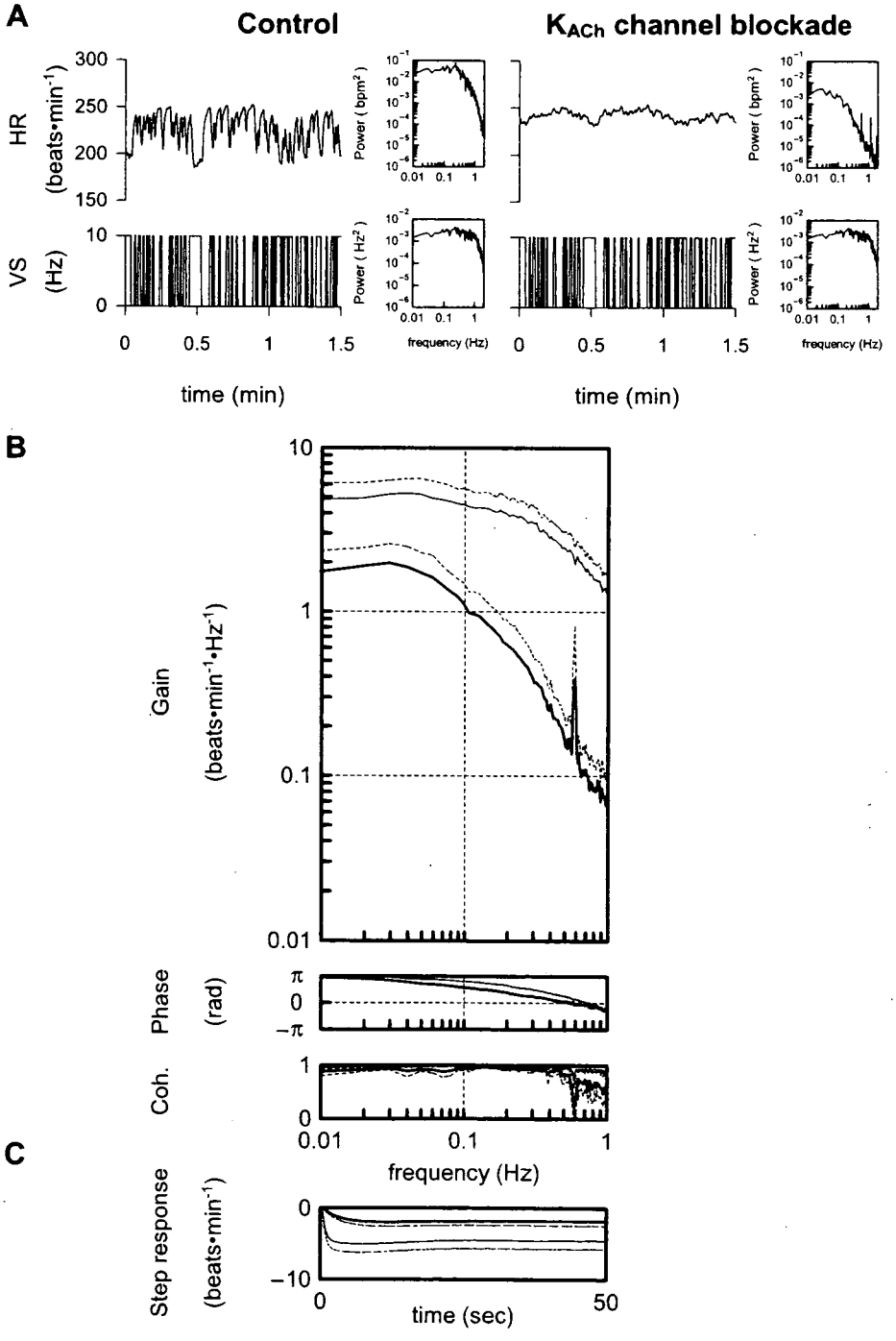

Fig. 1. *A*: representative recordings of heart rate (HR) obtained utilizing binary white-noise vagal stimulation (*top*) and corresponding vagal stimulation (VS, *bottom*). Traces were recorded before (control, *left*) and after tertiapin infusion (30 nmol/kg iv) for muscarinic K^+ (K_{ACh}) channel blockade (*right*). *Insets*: power spectra of each parameter. Tertiapin attenuated amplitude of HR variation and speed of response of HR to vagal stimulation. *B*: dynamic transfer function relating vagal stimulation to HR responses averaged from all animals (pooled data, $n = 9$). *Top*: gains; *middle*: phase shifts; *bottom*: coherence (Coh) functions. Frequency on abscissa (gain and phase) indicates frequency of input modulation, rather than stimulation frequency. *C*: calculated step response to 1-Hz tonic vagal stimulation averaged from all animals (pooled data, $n = 9$). Solid lines, means; dashed lines, SD. Thin line, control; thick line, K_{ACh} channel blockade with tertiapin (30 nmol/kg iv). Tertiapin decreased transfer gain and increased phase shift with increasing frequency, and tertiapin decreased maximum step response and slowed initial step response.

Table 1. *Effects of tertiapin infusion on AP and HR before and during dynamic vagal stimulation*

	Control	Tertiapin
AP, mmHg		
Before stimulation	82.4±20.5	77.6±20.7
During stimulation	77.9±20.0	74.8±18.6
HR, beats/min		
Before stimulation	247.3±24.7	248.1±32.7
During stimulation	212.4±22.3	231.1±25.9

Values are means ± SD (n = 9). Tertiapin was infused at 30 nmol/kg iv. AP, arterial pressure; HR, heart rate. Vagal stimulation significantly decreased HR ($P < 0.01$), but no significant effect of drug ($P = 0.28$) or interaction ($P = 0.32$) was observed by 2-way ANOVA.

more potent in the higher (>0.1 Hz) than in the lower frequency range.

Table 1 summarizes the mean values of AP and HR before and during vagal stimulation averaged from all animals. Dynamic vagal stimulation significantly decreased the mean HR ($P < 0.01$), but not the mean AP. Tertiapin did not significantly affect mean AP or HR before or during stimulation.

Figure 1*B* illustrates the dynamic transfer functions characterizing the vagal HR response averaged from all animals under control and tertiapin-mediated K_{ACh} channel blockade conditions. Gain plots, phase plots, and coherence functions are shown. Tertiapin attenuated the dynamic gain compared with the control conditions; the extent of the attenuation was greater in the higher frequency range: 63.0 ± 11.6, 74.4 ± 8.3, 93.0 ± 2.5, and 93.3 ± 3.9% at 0.01. 0.1, 0.5, and 1 Hz, respectively, as normalized to the control condition ($P < 0.01$ by ANOVA). The peak in the gain at 0.6 Hz observed during tertiapin-mediated K_{ATP} channel blockade would be caused by the artificial respiration (respiratory rate = 35–40 min^{-1}), because the low coherence value (~0.1) at 0.6 Hz indicates the independence of the input and output signals. This peak was masked by the large HR response to vagal stimulation under the control condition. The phase approached π radians at the lowest frequency and lagged with increasing frequency under the control condition; tertiapin caused the phase difference between the two conditions in the frequency range of 0.03–0.7 Hz, which disappeared at 1 Hz. The fitted parameters of the transfer functions are summarized in Table 2. Tertiapin significantly decreased the dynamic gain and the corner frequency without changing the lag time. Coherence was near unity in the overall frequency range in the control condition, whereas a decrease in the coherence function from unity was noted at >0.6 Hz with K_{ACh} channel blockade.

Figure 1*C* shows the calculated step response of HR to vagal stimulation averaged from all animals in the control condition and during K_{ACh} channel blockade. Tertiapin slowed the transient response (time constants = 0.6 ± 0.1 to 2.7 ± 0.5 s, $P < 0.01$) and attenuated the HR response to vagal stimulation (maximum step response = −4.5 ± 1.2 to −1.8 ± 0.6 beats/min, $P < 0.01$) in the time domain. Furthermore, tertiapin significantly delayed the 90% rise time of the step response, which was calculated as an index of system readiness (1.6 ± 0.5 to 5.0 ± 1.4 s, $P < 0.01$).

Static characteristics. Figure 2*A* shows typical recordings of step-wise vagal stimulation and the HR response in the control condition and during K_{ACh} channel blockade. The step-wise vagal stimulation decreased HR in a step-wise manner. Tertiapin attenuated the static reductions of HR from the baseline HR.

Figure 2*B* summarizes changes in HR in response to step-wise vagal stimulation. The step-wise vagal stimulation significantly decreased HR with increasing stimulus frequency under both conditions. Tertiapin significantly attenuated the static reductions of HR. The attenuation of HR reduction normalized to control conditions increased with increasing stimulus frequency: 45.8 ± 21.3, 58.2 ± 17.9, 64.7 ± 14.6, and 68.0 ± 11.4% at 5, 10, 15, and 20 Hz, respectively ($P < 0.05$ by ANOVA).

β-Adrenergic blockade protocol. In the supplemental protocol (n = 3) with β-adrenergic blockade, tertiapin decreased the dynamic gain from 2.4 ± 0.6 to 1.3 ± 0.5 beats·min^{-1}·Hz^{-1} and the corner frequency from 0.23 ± 0.05 to 0.06 ± 0.02 Hz without changing the lag time (0.36 ± 0.01 vs. 0.43 ± 0.00 s). In terms of the static characteristics, tertiapin significantly attenuated the vagal stimulation-induced HR decrease by 43 ± 10, 50 ± 8, 56 ± 7, and 61 ± 8% at stimulus frequencies of 5, 10, 15, and 20 Hz, respectively.

DISCUSSION

We have quantified the role of the K_{ACh} channels by examining the transfer characteristics. The major findings in the present study are that K_{ACh} channel blockade with intravenous tertiapin administration decreased the dynamic gain and corner frequency without changing the lag time of the dynamic transfer function from vagal stimulation to HR. These findings support our hypothesis that direct action of ACh via K_{ACh} channels contributes to the quickness of the HR control in response to electrical vagal stimulation.

Effect of tertiapin on dynamic transfer characteristics. Our results indicate that K_{ACh} channels contribute to a rapid component in vagal HR control. Tertiapin slowed the dynamic HR response to vagal stimulation, since tertiapin attenuated the gain of the transfer function significantly in the high frequency range (Fig. 1*B*). Moreover, the calculated step response clearly demonstrated this point (Fig. 1*C*). Tertiapin prolonged the time constant and 90% rise time of the step response by 2.1 and 3.4 s, respectively. Since quickness is a hallmark of the vagal control of HR relative to sympathetic control, these results highlight the importance of K_{ACh} channels in the rapidity of vagal HR control. Because tertiapin did not affect the lag time (Table 2), the increase in the 90% rise time to the step response due to tertiapin (~3.4 s) may primarily reflect the slowed transient response.

Our results are consistent with and may partly explain the earlier studies in which transgenic mice were used to investigate the role of K_{ACh} channels (8, 33). Using the G protein-

Table 2. *Effects of tertiapin infusion on parameters of the transfer function relating dynamic vagal stimulation to HR*

	Control	Tertiapin
Dynamic gain, beats·min^{-1}·Hz^{-1}	5.0±1.2	2.0±0.6*
Corner frequency, Hz	0.25±0.03	0.06±0.01*
Lag time, s	0.37±0.04	0.39±0.05

Values are means ± SD. Tertiapin was infused at 30 nmol/kg iv. *$P < 0.01$ vs. corresponding control.

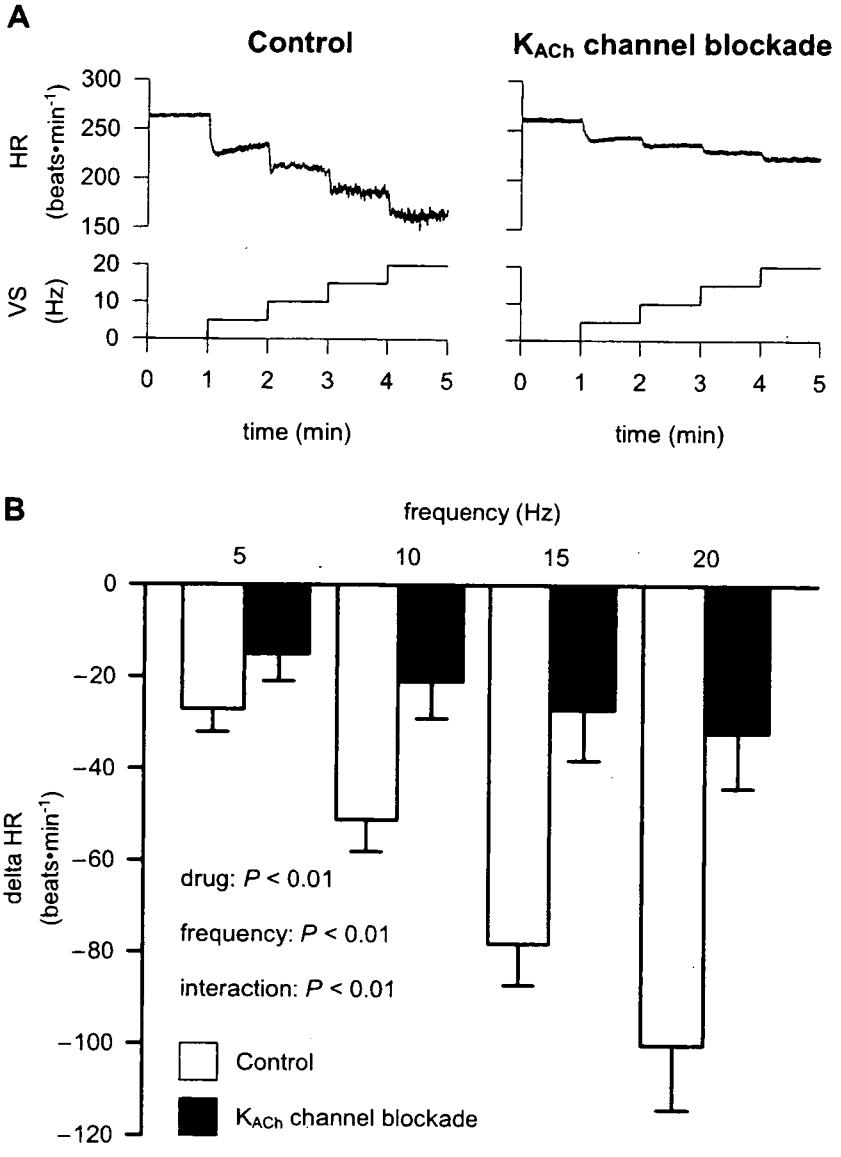

Fig. 2. *A*: representative recordings of HR (*top*) and corresponding vagal stimulation (*bottom*) obtained utilizing a step-wise stimulation. Traces were recorded before (control, *left*) and after tertiapin infusion (30 nmol/kg iv) for K_{ACh} channel blockade (*right*). K_{ACh} channel blockade attenuated amplitude of HR variation to tonic vagal stimulation. *B*: static transfer function relating step-wise vagal stimulation to HR responses averaged from all animals (pooled data, $n = 9$). Basal HR was not different between control and K_{ACh} channel blockade (see Table 1). K_{ACh} channel blockade decreases static HR response, and static reductions in bradycardic effect were greater at higher stimulation frequencies.

gated inwardly rectifying potassium (GIRK) channel family subunit GIRK4, which is a component of K_{ACh} channels (5, 16), Wickman et al. (33) indicated that the spectral power of HR was lower at 1.5–5.0 Hz, which is predominantly vagally mediated, but not at <0.4 Hz, in GIRK4-knockout than in wild-type mice. Another study using transgenic mice with a reduction in functional βγ-subunits of the G_i proteins also showed impaired vagal HR control, such as reductions in carbachol-induced bradycardia, HR variability, and baroreflex sensitivity (8). In the present study, tertiapin significantly attenuated the dynamic gain compared with the control conditions in the frequency bands from 0.01 to 1 Hz; the extent of the decreases in dynamic gain was augmented with increasing frequency of input modulation. This finding also supports the notion that K_{ACh} channels play a large part as a rapid component of vagal control of HR. Furthermore, increased phase shift due to tertiapin in the higher frequency range (0.03–0.7 Hz) would support the interpretation that the K_{ACh} channel current played an important role in the rapid HR response to vagal stimulation.

Tertiapin-mediated changes in fitted parameters of the transfer function from vagal stimulation to HR suggest that, at the postjunctional effector sites, the K_{ACh} channels play a key role in determining the dynamic properties of transduction from vagal nerve activity to HR. To quantitatively elucidate vagal and sympathetic control of HR, our research group used a transfer function analysis to examine the system characteristics. First, the transfer function from dynamic vagal nerve stimulation to HR approximated the characteristics of a first-order, low-pass filter, whereas the transfer function from dynamic sympathetic nerve stimulation to HR approximated the characteristics of a second-order, low-pass filter (14). Dynamic gain of vagal stimulation to HR was increased by concomitant sympathetic nerve stimulation (14) and pharmacologically induced accumulation of cAMP at the postjunctional effector sites (23) and decreased by high plasma norepinephrine (21). These perturbations of the indirect action of ACh did not affect the quickness of vagal HR control; i.e., neither corner frequency nor lag time was altered. On the contrary, inhibition of cholinesterase by neostigmine decreased the corner frequency

and increased the lag time (24). Taken together, these results might suggest that not only ACh kinetics at the neuroeffector site, but also the K_{ACh} channels at the postjunctional effector sites, play a key role in determining the dynamic properties of transduction from vagal nerve activity to HR.

Effect of tertiapin on the static transfer characteristics. Tertiapin attenuates the static reduction of HR in accord with the attenuation of the gain of the dynamic transfer function at the lowest frequency of input modulation. This suggests that K_{ACh} channels contribute to the static, as well as the rapid, component of vagal HR control. The relative attenuation of HR reduction increased with increasing stimulus frequency (Fig. 2*B*), suggesting that direct action of ACh in the static properties of transduction from vagus nerve activity to HR is augmented by an increase in the amount of available ACh. Although it is well established that the muscarinic response to static vagal stimulation depends on the stimulation frequency (26, 27), whether the contribution of the K_{ACh} channel pathway to the total HR response depends on the stimulus frequency remains unknown. The basal mean HR of GIRK-knockout mice (33) and transgenic mice with a reduction of βγ-subunits of the G_i proteins (8) is the same as that of wild-type mice, suggesting that K_{ACh} channels are not involved in mean HR control in the basal state. At low-to-moderate levels of vagal activity, vagal control of HR is due to changes in cAMP-modulated I_h, often referred to as "pacemaker" current (6). K_{ACh} channels might play an essential role in HR control at high levels of vagal activity.

In the present study, tertiapin decreased the HR response to vagal stimulation by ~70% of the control condition at a stimulus intensity of 20 Hz. This value is consistent with the earlier study by Yamada (34). This consistency suggested that K_{ACh} channels contribute to ~70% of the maximum negative chronotropic effects to pharmacologically and/or electronically induced vagal stimulation. However, changes in HR induced by tertiapin may have in turn affected the indirect action of ACh in the present study. Therefore, the percentage of direct vs. indirect action should be carefully interpreted.

Limitations. There are several limitations to this study. First, we did not confirm the completeness of K_{ACh} channel blockade. Kitamura et al. (15) demonstrated that tertiapin potently and selectively blocked the K_{ACh} channel in cardiac myocytes in a muscarinic receptor- and voltage-independent manner. Furthermore, Drici et al. (7) showed that tertiapin blocked K_{ACh} channels with an IC_{50} of ~30 nM with no significant effect on major currents associated with the cardiac repolarization process or atrioventricular conduction. On the basis of these studies, Hashimoto et al. (10) demonstrated that tertiapin (12 nmol/kg iv) significantly prolonged the atrial effective refractory period during vagal stimulation in their in vivo canine study. Therefore, we believe that the dose of tertiapin (30 nmol/kg iv) used in the present study should be sufficient to block K_{ACh} channel current in vivo.

Second, data were obtained from anesthetized animals. Since the anesthesia would affect the autonomic tone, the results may not be directly applicable to conscious animals. However, because we cut and stimulated the right cardiac vagal nerve, changes in autonomic outflow associated with anesthesia might not have significantly affected the results.

Third, in the present study, we stimulated the vagal nerve according to binary white noise and a step-wise pattern, which was quite different from the pattern of physiological neuronal discharge. However, although nonphysiological patterns of stimulation could theoretically bias the system identification results, because coherence was near unity over the frequency range of interest, by virtue of their inherent linearity, the system properties would not vary much with differing patterns of stimulation.

In conclusion, K_{ACh} channel blockade with intravenous tertiapin administration decreased the dynamic gain and corner frequency without changing the lag time of the transfer function from vagal stimulation to HR. In the time domain, tertiapin prolonged the time constant and 90% rise time of the step response. Additionally, tertiapin decreased the static reductions of HR from baseline HR to less than half of the control response with increasing vagal stimulus frequency. These results suggest that K_{ACh} channels accelerate the dynamic HR response to vagal stimulation and contribute more to the static HR response for more potent tonic vagal stimulation in vivo.

Perspectives

To simply identify the role of K_{ACh} channels in vagal HR control, a previous study (34) and the present study completely and/or partially excluded background sympathetic tone. However, in the physiological condition, sympathetic tone affects vagal control of HR and vice versa [e.g., accentuated antagonism (17)]. Pathophysiological conditions such as chronic heart failure (25), hypertension (19), and obesity (30) reveal increased basal sympathetic nerve activity compared with the normal condition. Tertiapin did not affect basal AP or HR (Table 1), suggesting that tertiapin did not affect sympathetic tone in the present experimental settings. Furthermore, under β-adrenergic blockade (the supplemental protocol), tertiapin decreased the dynamic gain and corner frequency, suggesting that the effects of tertiapin cannot be explained by the background sympathetic tone. However, the experimental design of the present study did not allow separate assessment of the direct vs. the indirect action of ACh, because the indirect action of ACh was not manipulated intentionally. Further investigation is needed to clarify the effects of sympathetic tone on the contribution of K_{ACh} channels to negative chronotropic effects.

GRANTS

This study was supported by Health and Labour Sciences Research Grants H15-Physi-001, H18-Nano-Ippan-003, and H18-Iryo-Ippan-023 from the Ministry of Health, Grant-in-Aid for Scientific Research promoted by the Ministry of Education, Culture, Sports, Science and Technology in Japan 18591992, and the Ground-Based Research Announcement for Space Utilization project promoted by the Japan Space Forum. This study was also supported by Industrial Technology Research Program Grant 06B44524a from the New Energy and Industrial Technology Development Organization of Japan.

REFERENCES

1. **Bendat J, Piersol A.** Single-input/output relationships. In: *Random Data Analysis and Measurement Procedures* (3rd ed). New York: Wiley, 2000, p. 189–217.
2. **Berger RD, Saul JP, Cohen RJ.** Transfer function analysis of autonomic regulation. I. Canine atrial rate response. *Am J Physiol Heart Circ Physiol* 256: H142–H152, 1989.
3. **Breitwieser GE, Szabo G.** Uncoupling of cardiac muscarinic and β-adrenergic receptors from ion channels by a guanine nucleotide analogue. *Nature* 317: 538–540, 1985.
4. **Brigham E.** FFT transform application. In: *The Fast Fourier Transform and Its Application.* Englewood Cliffs, NJ: Prentice-Hall, 1988, p. 167–203.

5. **Dascal N, Schreibmayer W, Lim NF, Wang W, Chavkin C, DiMagno L, Labarca C, Kieffer BL, Gaveriaux-Ruff C, Trollinger D, Lester HA, Davidson N.** Atrial G protein-activated K^+ channel: expression, cloning, and molecular properties. *Proc Natl Acad Sci USA* 90: 10235–10239, 1993.
6. **DiFrancesco D.** Cardiac pacemaker: 15 years of "new" interpretation. *Acta Cardiol* 50: 413–427, 1995.
7. **Drici MD, Diochot S, Terrenoire C, Romey G, Lazdunski M.** The bee venom peptide tertiapin underlines the role of $I_{K\,ACh}$ in acetylcholine-induced atrioventricular blocks. *Br J Pharmacol* 131: 569–577, 2000.
8. **Gehrmann J, Meister M, Maguire CT, Martins DC, Hammer PE, Neer EJ, Berul CI, Mende U.** Impaired parasympathetic heart rate control in mice with a reduction of functional G protein βγ-subunits. *Am J Physiol Heart Circ Physiol* 282: H445–H456, 2002.
9. **Hartzell HC, Mery PF, Fischmeister R, Szabo G.** Sympathetic regulation of cardiac calcium current is due exclusively to cAMP-dependent phosphorylation. *Nature* 351: 573–576, 1991.
10. **Hashimoto N, Yamashita T, Tsuruzoe N.** Tertiapin, a selective $I_{K\,ACh}$ blocker, terminates atrial fibrillation with selective atrial effective refractory period prolongation. *Pharmacol Res* 54: 136–141, 2006.
11. **Huang CL, Slesinger PA, Casey PJ, Jan YN, Jan LY.** Evidence that direct binding of Gβγ to the GIRK1 G protein-gated inwardly rectifying K^+ channel is important for channel activation. *Neuron* 15: 1133–1143, 1995.
12. **Irisawa H, Brown HF, Giles W.** Cardiac pacemaking in the sinoatrial node. *Physiol Rev* 73: 197–227, 1993.
13. **Jin W, Lu Z.** Synthesis of a stable form of tertiapin: a high-affinity inhibitor for inward-rectifier K^+ channels. *Biochemistry* 38: 14286–14293, 1999.
14. **Kawada T, Ikeda Y, Sugimachi M, Shishido T, Kawaguchi O, Yamazaki T, Alexander J Jr, Sunagawa K.** Bidirectional augmentation of heart rate regulation by autonomic nervous system in rabbits. *Am J Physiol Heart Circ Physiol* 271: H288–H295, 1996.
15. **Kitamura H, Yokoyama M, Akita H, Matsushita K, Kurachi Y, Yamada M.** Tertiapin potently and selectively blocks muscarinic K^+ channels in rabbit cardiac myocytes. *J Pharmacol Exp Ther* 293: 196–205, 2000.
16. **Krapivinsky G, Gordon EA, Wickman K, Velimirovic B, Krapivinsky L, Clapham DE.** The G-protein-gated atrial K^+ channel $I_{K\,ACh}$ is a heteromultimer of two inwardly rectifying K^+-channel proteins. *Nature* 374: 135–141, 1995.
17. **Levy MN.** Sympathetic-parasympathetic interactions in the heart. *Circ Res* 29: 437–445, 1971.
18. **Luetje CW, Tietje KM, Christian JL, Nathanson NM.** Differential tissue expression and developmental regulation of guanine nucleotide binding regulatory proteins and their messenger RNAs in rat heart. *J Biol Chem* 263: 13357–13365, 1988.
19. **Mancia G, Grassi G, Giannattasio C, Seravalle G.** Sympathetic activation in the pathogenesis of hypertension and progression of organ damage. *Hypertension* 34: 724–728, 1999.
20. **Marmarelis P, Marmarelis V.** The white noise method in system identification. In: *Analysis of Physiological Systems*. New York: Plenum, 1978, p. 131–221.
21. **Miyamoto T, Kawada T, Takaki H, Inagaki M, Yanagiya Y, Jin Y, Sugimachi M, Sunagawa K.** High plasma norepinephrine attenuates the dynamic heart rate response to vagal stimulation. *Am J Physiol Heart Circ Physiol* 284: H2412–H2418, 2003.
22. **Miyamoto T, Kawada T, Yanagiya Y, Inagaki M, Takaki H, Sugimachi M, Sunagawa K.** Cardiac sympathetic nerve stimulation does not attenuate dynamic vagal control of heart rate via α-adrenergic mechanism. *Am J Physiol Heart Circ Physiol* 287: H860–H865, 2004.
23. **Nakahara T, Kawada T, Sugimachi M, Miyano H, Sato T, Shishido T, Yoshimura R, Miyashita H, Inagaki M, Alexander J Jr, Sunagawa K.** Accumulation of cAMP augments dynamic vagal control of heart rate. *Am J Physiol Heart Circ Physiol* 275: H562–H567, 1998.
24. **Nakahara T, Kawada T, Sugimachi M, Miyano H, Sato T, Shishido T, Yoshimura R, Miyashita H, Sunagawa K.** Cholinesterase affects dynamic transduction properties from vagal stimulation to heart rate. *Am J Physiol Regul Integr Comp Physiol* 275: R541–R547, 1998.
25. **Negrao CE, Rondon MU, Tinucci T, Alves MJ, Roveda F, Braga AM, Reis SF, Nastari L, Barretto AC, Krieger EM, Middlekauff HR.** Abnormal neurovascular control during exercise is linked to heart failure severity. *Am J Physiol Heart Circ Physiol* 280: H1286–H1292, 2001.
26. **Parker P, Celler BG, Potter EK, McCloskey DI.** Vagal stimulation and cardiac slowing. *J Auton Nerv Syst* 11: 226–231, 1984.
27. **Priola DV, Cote I.** Differential sensitivity of the canine heart to acetylcholine and vagal stimulation. *Am J Physiol Heart Circ Physiol* 234: H460–H464, 1978.
28. **Sakmann B, Noma A, Trautwein W.** Acetylcholine activation of single muscarinic K^+ channels in isolated pacemaker cells of the mammalian heart. *Nature* 303: 250–253, 1983.
29. **Saul JP, Berger RD, Albrecht P, Stein SP, Chen MH, Cohen RJ.** Transfer function analysis of the circulation: unique insights into cardiovascular regulation. *Am J Physiol Heart Circ Physiol* 261: H1231–H1245, 1991.
30. **Seals DR, Bell C.** Chronic sympathetic activation: consequence and cause of age-associated obesity? *Diabetes* 53: 276–284, 2004.
31. **Spear JF, Moore EN.** Influence of brief vagal and stellate nerve stimulation on pacemaker activity and conduction within the atrioventricular conduction system of the dog. *Circ Res* 32: 27–41, 1973.
32. **Sunahara RK, Dessauer CW, Gilman AG.** Complexity and diversity of mammalian adenylyl cyclases. *Annu Rev Pharmacol Toxicol* 36: 461–480, 1996.
33. **Wickman K, Nemec J, Gendler SJ, Clapham DE.** Abnormal heart rate regulation in GIRK4 knockout mice. *Neuron* 20: 103–114, 1998.
34. **Yamada M.** The role of muscarinic K^+ channels in the negative chronotropic effect of a muscarinic agonist. *J Pharmacol Exp Ther* 300: 681–687, 2002.
35. **Yamada M, Inanobe A, Kurachi Y.** G protein regulation of potassium ion channels. *Pharmacol Rev* 50: 723–760, 1998.

J Appl Physiol 102: 622–627, 2007.
First published November 2, 2006; doi:10.1152/japplphysiol.00622.2006.

Hypothermia reduces ischemia- and stimulation-induced myocardial interstitial norepinephrine and acetylcholine releases

Toru Kawada,[1] Hirotoshi Kitagawa,[2] Toji Yamazaki,[2] Tsuyoshi Akiyama,[2] Atsunori Kamiya,[1] Kazunori Uemura,[1] Hidezo Mori,[2] and Masaru Sugimachi[1]

[1]*Department of Cardiovascular Dynamics, Advanced Medical Engineering Center, and*
[2]*Department of Cardiac Physiology, National Cardiovascular Center Research Institute, Osaka, Japan*

Submitted 4 June 2006; accepted in final form 1 November 2006

Kawada T, Kitagawa H, Yamazaki T, Akiyama T, Kamiya A, Uemura K, Mori H, Sugimachi M. Hypothermia reduces ischemia- and stimulation-induced myocardial interstitial norepinephrine and acetylcholine releases. *J Appl Physiol* 102: 622–627, 2007. First published November 2, 2006; doi:10.1152/japplphysiol.00622.2006.—Although hypothermia is one of the most powerful modulators that can reduce ischemic injury, the effects of hypothermia on the function of the cardiac autonomic nerves in vivo are not well understood. We examined the effects of hypothermia on the myocardial interstitial norepinephrine (NE) and ACh releases in response to acute myocardial ischemia and to efferent sympathetic or vagal nerve stimulation in anesthetized cats. We induced acute myocardial ischemia by coronary artery occlusion. Compared with normothermia ($n = 8$), hypothermia at 33°C ($n = 6$) suppressed the ischemia-induced NE release [63 nM (SD 39) vs. 18 nM (SD 25), $P < 0.01$] and ACh release [11.6 nM (SD 7.6) vs. 2.4 nM (SD 1.3), $P < 0.01$] in the ischemic region. Under hypothermia, the coronary occlusion increased the ACh level from 0.67 nM (SD 0.44) to 6.0 nM (SD 6.0) ($P < 0.05$) and decreased the NE level from 0.63 nM (SD 0.19) to 0.40 nM (SD 0.25) ($P < 0.05$) in the nonischemic region. Hypothermia attenuated the nerve stimulation-induced NE release from 1.05 nM (SD 0.85) to 0.73 nM (SD 0.73) ($P < 0.05$, $n = 6$) and ACh release from 10.2 nM (SD 5.1) to 7.1 nM (SD 3.4) ($P < 0.05$, $n = 5$). In conclusion, hypothermia attenuated the ischemia-induced NE and ACh releases in the ischemic region. Moreover, hypothermia also attenuated the nerve stimulation-induced NE and ACh releases. The Bezold-Jarisch reflex evoked by the left anterior descending coronary artery occlusion, however, did not appear to be affected under hypothermia.

vagal nerve; sympathetic nerve; cardiac microdialysis; cats

HYPOTHERMIA IS ONE OF THE most powerful modulators that can reduce ischemic injury in the central nervous system, heart, and other organs. The general consensus is that hypothermia induces a hypometabolic state in tissues and balances energy supply and demand (25). With respect to the myocardial ischemia, the size of a myocardial infarction correlates with temperature (6), and mild hypothermia can protect the myocardium against acute ischemic injury (9). The effects of hypothermia on the function of the cardiac autonomic nerves in terms of neurotransmitter releases, however, are not fully understood. Because autonomic neurotransmitters such as norepinephrine (NE) and ACh directly impinge on the myocardium, they would be implicated in the cardioprotection by hypothermia.

In previous studies from our laboratory, Kitagawa et al. (16) demonstrated that hypothermia attenuated the nonexocytotic NE release induced pharmacologically by ouabain, tyramine, or cyanide. Kitagawa et al. (15) also demonstrated that hypothermia attenuated the exocytotic NE release in response to vena cava occlusion or to local administration of high K^+. The effects of hypothermia on the ischemia-induced myocardial interstitial NE release, however, were not examined in those studies. In addition, the effects of hypothermia on the ischemia-induced myocardial interstitial ACh release have never been examined. Because both sympathetic and parasympathetic nerves control the heart, simultaneous monitoring of the myocardial interstitial releases of NE and ACh (14, 31) would help integrative understanding of the autonomic nerve terminal function under hypothermia in conjunction with acute myocardial ischemia.

In the present study, the effects of hypothermia on the ischemia-induced and nerve stimulation-induced myocardial interstitial neurotransmitter releases were examined. We implanted a dialysis probe into the left ventricular free wall of anesthetized cats and measured dialysate NE and ACh levels as indexes of neurotransmitter outputs from the cardiac sympathetic and vagal nerve terminals, respectively. Based on our laboratory's previous results (15, 16), we hypothesized that hypothermia would attenuate the neurotransmitter releases in response to acute myocardial ischemia and to electrical nerve stimulation.

MATERIALS AND METHODS

Surgical Preparation and Protocols

Animals were cared for in accordance with the *Guiding Principles for the Care and Use of Animals in the Field of Physiological Sciences*, approved by the Physiological Society of Japan. All protocols were reviewed and approved by the Animal Subjects Committee of National Cardiovascular Center. Adult cats were anesthetized via an intraperitoneal injection of pentobarbital sodium (30–35 mg/kg) and ventilated mechanically through an endotracheal tube with oxygen-enriched room air. The level of anesthesia was maintained with a continuous intravenous infusion of pentobarbital sodium (1–2 $mg \cdot kg^{-1} \cdot h^{-1}$) through a catheter inserted from the right femoral vein. Mean arterial pressure (MAP) was measured using a pressure transducer connected to a catheter inserted from the right femoral artery. Heart rate (HR) was determined from an electrocardiogram.

Protocol 1: acute myocardial ischemia. We examined the effects of hypothermia on the ischemia-induced myocardial interstitial releases of NE and ACh. The heart was exposed by partially removing the left fifth and/or sixth rib. A dialysis probe was implanted transversely into

Address for reprint requests and other correspondence: T. Kawada, Dept. of Cardiovascular Dynamics, Advanced Medical Engineering Center, National Cardiovascular Center Research Institute, 5-7-1 Fujishirodai, Suita, Osaka 565-8565, Japan (e-mail: torukawa@res.ncvc.go.jp).

The costs of publication of this article were defrayed in part by the payment of page charges. The article must therefore be hereby marked "*advertisement*" in accordance with 18 U.S.C. Section 1734 solely to indicate this fact.

the anterolateral free wall of the left ventricle perfused by the left anterior descending coronary artery (LAD) to monitor myocardial interstitial NE and ACh levels in the ischemic region during occlusion of the LAD (13). Another dialysis probe was implanted transversely into the posterior free wall of the left ventricle perfused by the left circumflex coronary artery to monitor myocardial interstitial NE and ACh levels in a nonischemic region. Heparin sodium (100 U/kg) was administered intravenously to prevent blood coagulation. Animals were divided into a normothermic group (n = 8) and a hypothermic group (n = 6). In the hypothermic group, surface cooling with ice bags was performed until the esophageal temperature decreased to 33°C (15, 16). A stable hypothermic condition was obtained within ~2 h. In each group, we occluded the LAD for 60 min and examined changes in the myocardial interstitial NE and ACh levels in the ischemic region (i.e., the LAD region) and nonischemic region (i.e., the left circumflex coronary artery region). Fifteen-minute dialysate samples were obtained during the preocclusion baseline condition and during the periods of 0–15, 15–30, 30–45, and 45–60 min of the LAD occlusion.

Protocol 2: sympathetic stimulation. We examined the effects of hypothermia on the sympathetic nerve stimulation-induced myocardial interstitial NE release (n = 6). A dialysis probe was implanted transversely into the anterolateral free wall of the left ventricle. The bilateral cardiac sympathetic nerves originating from the stellate ganglia were exposed through a second intercostal space and sectioned. The cardiac end of each sectioned nerve was placed on a bipolar platinum electrode for sympathetic stimulation (5 Hz, 10 V, 1-ms pulse duration). The electrodes and nerves were covered with mineral oil to provide insulation and prevent desiccation. A 4-min dialysate sample was obtained during the sympathetic stimulation under the normothermic condition. Thereafter, hypothermia was introduced using the same cooling procedure as in *protocol 1*, and a second 4-min dialysate sample was obtained during the sympathetic stimulation.

Protocol 3: vagal stimulation. We examined the effects of hypothermia on the vagal nerve stimulation-induced ACh release (n = 5). A dialysis probe was implanted transversely into the anterolateral free wall of the left ventricle. The bilateral vagi were exposed through a midline cervical incision and sectioned at the neck. The cardiac end of each sectioned nerve was placed on a bipolar platinum electrode for vagal stimulation (20 Hz, 10 V, 1-ms pulse duration). To prevent severe bradycardia and cardiac arrest, which can be induced by the vagal stimulation, the heart was paced at 200 beats/min using pacing wires attached to the apex of the heart during the stimulation period. A 4-min dialysate sample was obtained during the vagal stimulation under the normothermic condition. Thereafter, hypothermia was introduced using the same cooling procedure as in *protocol 1*, and a second 4-min dialysate sample was obtained during the vagal stimulation.

Because of the relatively intense stimulation of the sympathetic or vagal nerve, the stimulation period in *protocols 2* and *3* was limited to 4 min to minimize gradual waning of the stimulation effects. At the end of the experiment, the animals were killed by increasing the depth of anesthesia with an overdose of pentobarbital sodium. We then confirmed that the dialysis probes had been threaded in the middle layer of the left ventricular myocardium.

Dialysis Technique

The dialysate NE and ACh concentrations were measured as indexes of myocardial interstitial NE and ACh levels, respectively. The materials and properties of the dialysis probe have been described previously (2, 3). Briefly, we designed a transverse dialysis probe. A dialysis fiber (13-mm length, 310-μm outer diameter, 200-μm inner diameter; PAN-1200, 50,000 molecular weight cutoff; Asahi Chemical) was connected at both ends to polyethylene tubes (25-cm length, 500-μm outer diameter, 200-μm inner diameter). The dialysis probe was perfused with Ringer solution containing a cholinesterase inhibitor eserine (10^{-4} M) at a rate of 2 μl/min. We started dialysate sampling from 2 h after the implantation of the dialysis probe(s), when the dialysate NE and ACh concentrations had reached steady states. The actual dialysate sampling was delayed by 5 min from the collection period to account for the dead space volume between the semipermeable membrane and the sample tube. Each sample was collected in a microtube containing 3 μl of HCl to prevent amine oxidation. The dialysate ACh concentration was measured directly by HPLC with electrochemical detection (Eicom). The in vitro recovery rate of ACh was ~70%. With the use of a criterion of signal-to-noise ratio of higher than three, the detection limit for ACh was 3 pg per injection. The dialysate NE concentration was measured by another HPLC-electrochemical detection system after the removal of interfering compounds by an alumina procedure. The in vitro recovery rate of NE was ~55%. With the use of a criterion of signal-to-noise ratio of higher than three, the detection limit for NE was 200 fg per injection.

Statistical Analysis

All data are presented as means and SD values. For *protocol 1*, we performed two-way repeated-measures ANOVA using hypothermia as one factor and the dialysate sampling periods (the effects of ischemia) as the other factor. For *protocols 2* and *3*, we compared stimulation-induced releases of NE and ACh before and during hypothermia using a paired t-test. For all of the statistics, the difference was considered significant when $P < 0.05$.

RESULTS

Figure 1*A* illustrates changes in myocardial interstitial NE levels in the ischemic region during LAD occlusion obtained from *protocol 1*. The *inset* shows the magnified ordinate for the

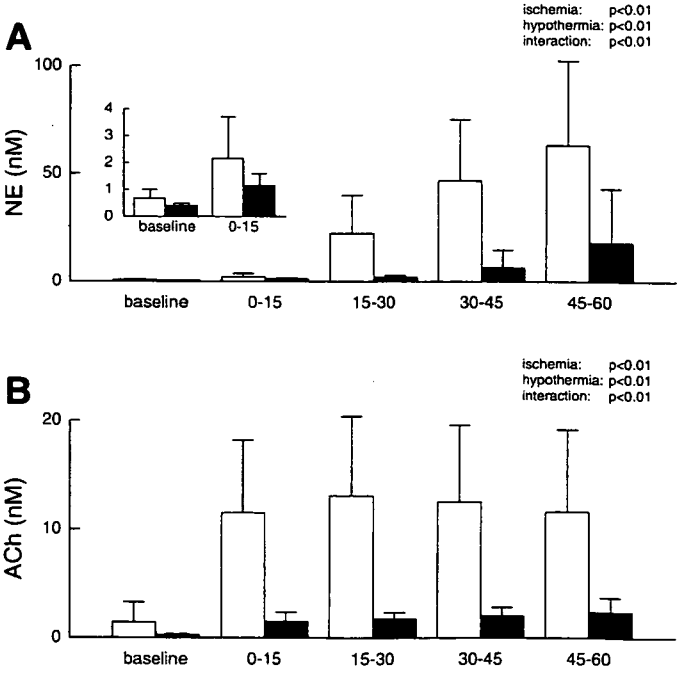

Fig. 1. *A*: ischemia-induced myocardial interstitial norepinephrine (NE) release in the ischemic region. Acute myocardial ischemia caused a progressive increase in the level of myocardial interstitial NE. Hypothermia attenuated the ischemia-induced NE release. *Inset*: magnified ordinate for the baseline and the 0- to 15-min period of ischemia. *B*: ischemia-induced myocardial interstitial ACh release in the ischemic region. Acute myocardial ischemia increased the myocardial interstitial ACh levels. Hypothermia attenuated the ischemia-induced ACh release. Open bars: normothermia; solid bars: hypothermia.

baseline and the 0- to 15-min period of ischemia. In the normothermic group (open bars), the LAD occlusion caused an ~94-fold increase in the NE level during the 45- to 60-min interval. In the hypothermic group (solid bars), the LAD occlusion caused an ~45-fold increase in the NE level during the 45- to 60-min interval. Compared with normothermia, hypothermia suppressed the baseline NE level to ~59% and the NE level during the 45- to 60-min period to ~29%. Statistical analysis indicated that the effects of both hypothermia and ischemia on the NE release were significant, and the interaction between hypothermia and ischemia was also significant.

Figure 1*B* illustrates changes in myocardial interstitial ACh levels in the ischemic region during the LAD occlusion. In both the normothermic (open bars) and hypothermic (solid bars) groups, the LAD occlusion caused an approximately eightfold increase in the ACh level during the 45- to 60-min interval. Compared with normothermia, however, hypothermia suppressed both the baseline ACh level and the ACh level during the 45- to 60-min period of ischemia to ~20%. Statistical analysis indicated that the effects of both hypothermia and ischemia on the ACh release were significant, and the interaction between hypothermia and ischemia was also significant.

Figure 2*A* illustrates changes in myocardial interstitial NE levels in the nonischemic region during the LAD occlusion. Note that scale of the ordinate is only one-hundredth of that in Fig. 1*A*. The LAD occlusion decreased the NE level in the normothermic group (open bars); the NE level during the 45- to 60-min interval was ~59% of the baseline level. The LAD occlusion also decreased the NE level in the hypothermic group (solid bars); the NE level during the 45- to 60-min interval was ~64% of the baseline level. Although the LAD occlusion resulted in a decrease in the NE level under both conditions, the NE level under hypothermia was nearly twice that measured under normothermia. The statistical analysis indicated that the effects of both hypothermia and ischemia on the NE release were significant, whereas the interaction between hypothermia and ischemia was not significant.

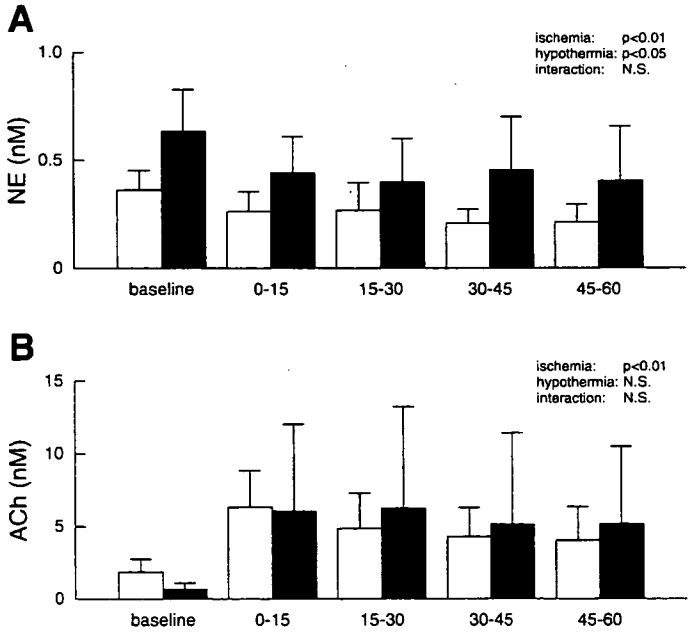

Fig. 2. *A*: changes in the myocardial interstitial NE levels in the nonischemic region. Acute myocardial ischemia decreased the level of myocardial interstitial NE from the baseline level. Hypothermia increased the myocardial interstitial NE levels in the nonischemic region. *B*: changes in the myocardial interstitial ACh levels in the nonischemic region. Acute myocardial ischemia increased the myocardial interstitial ACh level. Hypothermia did not attenuate the increasing response of ACh to the left anterior descending coronary artery occlusion. Open bars: normothermia; solid bars: hypothermia. NS, not significant.

Table 1. *Mean arterial pressure during acute myocardial ischemia obtained in protocol 1*

	Baseline	5 min	15 min	30 min	45 min	60 min
Normothermia	108 (23)	102 (28)	101 (24)	101 (20)	102 (21)	102 (21)
Hypothermia	108 (11)	80 (17)	87 (10)	85 (10)	86 (10)	91 (11)

Values are means (SD) (in mmHg) obtained during preocclusion baseline period and 5-, 15-, 30-, 45-, and 60-min periods of coronary artery occlusion. Ischemia: $P < 0.01$; hypothermia: not significant; interaction: $P < 0.01$.

Figure 2*B* illustrates changes in myocardial interstitial ACh levels in the nonischemic region during the LAD occlusion. The LAD occlusion caused an ~3.4-fold increase in the ACh level during the 0- to 15-min interval in the normothermic group (open bars). The LAD occlusion caused an approximately ninefold increase in the ACh level during the 0- to 15-min interval in the hypothermic group (solid bars). These effects of ischemia on the ACh release were statistically significant. Although hypothermia seemed to attenuate the baseline ACh level, the overall effects of hypothermia on the ACh level were insignificant.

Tables 1 and 2 summarize the MAP and HR data, respectively, obtained in *protocol 1*. Acute myocardial ischemia significantly reduced MAP ($P < 0.01$) and HR ($P < 0.01$). Hypothermia did not affect MAP but did decrease HR ($P < 0.01$). The interaction between ischemia and hypothermia was significant for MAP but not for HR by the two-way repeated-measures ANOVA.

For *protocol 2*, hypothermia significantly attenuated the sympathetic stimulation-induced NE release to ~70% of the level observed during normothermia (Fig. 3*A*). Under normothermia, the sympathetic stimulation increased MAP from 114 mmHg (SD 27) to 134 mmHg (SD 33) ($P < 0.01$) and HR from 147 beats/min (SD 9) to 207 beats/min (SD 5) ($P < 0.01$). Under hypothermia, the sympathetic stimulation increased MAP from 117 mmHg (SD 11) to 136 mmHg (SD 22) ($P < 0.05$) and HR from 125 beats/min (SD 16) to 164 beats/min (SD 10) ($P < 0.01$).

For *protocol 3*, hypothermia significantly attenuated the vagal stimulation-induced ACh release to ~70% of the level observed during normothermia (Fig. 3*B*). Hypothermia did not change MAP [117 mmHg (SD 18) vs. 118 mmHg (SD 27)] but

Table 2. *Heart rate during acute myocardial ischemia obtained in protocol 1*

	Baseline	5 min	15 min	30 min	45 min	60 min
Normothermia	183 (26)	160 (18)	163 (16)	163 (18)	166 (20)	165 (21)
Hypothermia	146 (25)	116 (19)	113 (19)	126 (39)	112 (20)	97 (31)

Values are means (SD) (in beats/min) obtained during preocclusion baseline period and 5-, 15-, 30-, 45-, and 60-min periods of coronary artery occlusion. Ischemia: $P < 0.01$; hypothermia: $P < 0.01$; interaction: not significant.

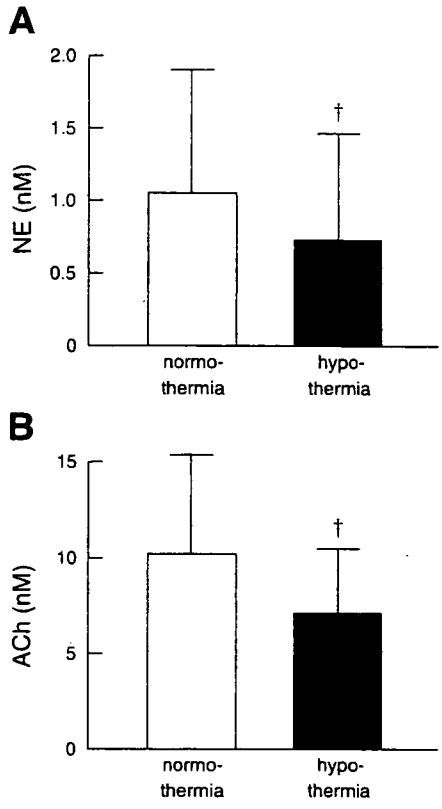

Fig. 3. *A*: efferent sympathetic nerve stimulation-induced release of myocardial interstitial NE before and during hypothermia. †Hypothermia significantly attenuated the stimulation-induced NE release. *B*: efferent vagal nerve stimulation-induced release of myocardial interstitial ACh before and during hypothermia. †Hypothermia significantly attenuated the stimulation-induced ACh release.

did decrease HR from 202 beats/min (SD 24) to 179 beats/min (SD 15) ($P < 0.05$) during the prestimulation, unpaced condition. MAP during the stimulation was 105 mmHg (SD 19) under normothermia and 93 mmHg (SD 33) under hypothermia.

DISCUSSION

A cardiac microdialysis is a powerful tool to estimate neurotransmitter levels in the myocardial interstitium in vivo (2, 3, 14, 19, 20, 31). The present study demonstrated that hypothermia significantly attenuated the myocardial interstitial releases of NE and ACh in the ischemic region during the LAD occlusion. In contrast, the increasing response in the ACh level from its baseline level and the decreasing response in the NE level from its baseline level observed in the nonischemic region were maintained under hypothermia. To our knowledge, this is the first report showing the effects of hypothermia on the myocardial interstitial releases of NE and ACh during acute myocardial ischemia in vivo. In addition, the present study showed that hypothermia significantly attenuated nerve stimulation-induced myocardial interstitial NE and ACh releases in vivo.

Effects of Hypothermia on Ischemia-induced NE and ACh Releases in the Ischemic Region

Acute myocardial ischemia causes energy depletion, which leads to myocardial interstitial NE release in the ischemic region (Fig. 1*A*). The NE release can be classified as exocytotic or nonexocytotic (18, 24). Exocytotic release indicates NE release from synaptic vesicles, which normally occurs in response to nerve discharge and subsequent Ca^{2+} influx through voltage-dependent Ca^{2+} channels. On the other hand, nonexocytotic release indicates NE release from the axoplasm, such as that mediated by a reverse transport through the NE transporter. A neuronal uptake blocker, desipramine, can suppress the ischemia-induced NE release (19, 24). Whereas exocytotic release contributes to the ischemia-induced NE release in the initial phase of ischemia (within ~20 min), carrier-mediated nonexocytotic release becomes predominant as the ischemic period is prolonged (1). Hypothermia significantly attenuated the ischemia-induced NE release (Fig. 1*A*). The NE level during the 45- to 60-min period of ischemia under hypothermia was ~20% of that obtained under normothermia. The NE uptake transporter is driven by the Na^+ gradient across the cell membrane (23). The loss of the Na^+ gradient due to ischemia causes NE to be transported out of the cell by reversing the action of the NE transporter. Hypothermia inhibits the action of the NE transporter and also suppresses the intracellular Na^+ accumulation (8), thereby reducing nonexocytotic NE release during ischemia. The present results are in line with an in vitro study that showed hypothermia suppressed nonexocytotic NE release induced by deprivation of oxygen and glucose (30). The present results are also consistent with a previous study from our laboratory that showed hypothermia attenuated the nonexocytotic NE release induced by ouabain, tyramine, or cyanide (16).

Acute myocardial ischemia increases myocardial interstitial ACh level in the ischemic region, as reported previously (Fig. 1*B*) (13). The level of ischemia-induced ACh release during 0- to 15-, 15- to 30-, 30- to 45-, or 45- to 60-min period of ischemia is comparable to that evoked by 4-min electrical stimulation of the bilateral vagi (Fig. 3*B*). Compared with the normothermic condition, hypothermia significantly attenuated the ischemia-induced myocardial interstitial release of ACh in the ischemic region. Our laboratory's previous study indicated that intracellular Ca^{2+} mobilization is essential for the ischemia-induced release of ACh (13). Hypothermia may have prevented the Ca^{2+} overload, thereby reducing the ischemia-induced ACh release. Alternatively, hypothermia may reduce the extent of the ischemic injury, which in turn suppressed the ischemia-induced ACh release. Because ACh has protective effects on the cardiomyocytes against ischemia (11), the suppression of ischemia-induced ACh release during hypothermia itself may be unfavorable for cardioprotection.

There is considerable controversy regarding the cardioprotective effects of β-adrenergic blockade during severe ischemia, with studies demonstrating a reduction of infarct size (10, 17) or no effects (7, 27). The β-adrenergic blockade seems effective to protect the heart only when the heart is reperfused within a certain period after the coronary occlusion. The β-adrenergic blockade would reduce the myocardial oxygen consumption through the reduction of HR and ventricular contractility and delay the progression of ischemic injury. Hence the infarct size might be reduced when the heart is reperfused before the ischemic damage becomes irreversible. The ischemia-induced NE release reached nearly 100 times the baseline NE level under normothermia (Fig. 1*A*), which by far exceeded the NE level attained by electrical stimulation of the

bilateral stellate ganglia (Fig. 3*A*). Because high NE levels have cardiotoxic effects (22), ischemia-induced NE release might aggravate the ischemic injury. However, catecholamine depletion by a reserpine treatment fails to reduce the infarct size (26, 29), throwing a doubt on the involvement of catecholamine toxicity in the progression of myocardial damage during ischemia. It is, therefore, most likely that the hypothermia-induced reductions in NE and ACh are the result of reduced myocardial damage or a direct effect on nerve endings.

Van den Doel et al. (28) showed that hypothermia does not abolish necrosis, but rather delays necrosis during sustained ischemia, so that hypothermia protected against infarction produced by a 30-min occlusion but not against infarction produced by a 60-min occlusion in the rat heart. At the same time, they mentioned that hypothermia was able to reduce the infarct size after a 60-min coronary occlusion in the dog, possibly because of the significant collateral flow in the canine hearts. Because the feline hearts are similar to the canine hearts in that they have considerable collateral flow compared with the rat hearts (21), hypothermia should have protected the feline heart against the 60-min coronary occlusion in the present study.

Effects of Hypothermia on the NE and ACh Releases in the Nonischemic Region and on the Electrical Stimulation-induced NE and ACh Releases

The NE and ACh levels in the nonischemic region may reflect the sympathetic and parasympathetic drives to this region. As an example, myocardial interstitial ACh levels increase during activations of the arterial baroreflex and the Bezold-Jarisch reflex (14). In the present study, acute myocardial ischemia decreased the NE level from its baseline level, whereas it increased the ACh level from its baseline level (Fig. 2). Ischemia also decreased MAP and HR (Tables 1 and 2), suggesting that the Bezold-Jarisch reflex was induced by the LAD occlusion under both normothermia and hypothermia. Taking into account the fact that electrical stimulation-induced ACh release was attenuated to ~70% (Fig. 3), similar ACh levels during ischemia imply the enhancement of the parasympathetic outflow via the Bezold-Jarisch reflex under hypothermia. These results are in line with the study by Zheng et al. (32), where pulmonary chemoreflex-induced bradycardia was maintained under hypothermia. Hypothermia increased the NE level in the nonischemic region, suggesting that sympathetic drive to this region also increased. Hypothermic stress is known to cause sympathetic activation, accompanying increases in MAP, HR, plasma NE, and epinephrine levels (4). In the present study, because the effect of hypothermia on MAP was insignificant (Table 1) and HR decreased under hypothermia (Table 2), the sympathetic activation observed in the nonischemic region might have been regional and not systemic.

Hypothermia attenuated the releases of NE and ACh in response to respective nerve stimulation to ~70% of that observed under normothermia (Fig. 3). The suppression of the exocytotic NE release by hypothermia is consistent with a previous study from our laboratory, where hypothermia attenuated the myocardial interstitial NE release in response to vena cava occlusion or to a local high K^+ administration (15). The suppression of NE release by hypothermia is consistent with an in vitro study by Kao and Westhead (12) in which catecholamine secretion from adrenal chromaffin cells induced by elevated K^+ levels increased as the temperature increased from 4 to 37°C. On the other hand, because hypothermia inhibits the neuronal NE uptake, the NE concentration at the synaptic cleft is expected to be increased if the level of NE release remains unchanged. Actually, Vizi (30) demonstrated that hypothermia increased NE release in response to field stimulation in vitro. In the present study, however, the suppression of NE release might have canceled the potential accumulation of NE due to NE uptake inhibition. The present study also demonstrated that the ACh release was suppressed by hypothermia. In the rat striatum, hypothermia decreases the extracellular ACh concentration and increases the choline concentration (5). Hypothermia may inhibit a choline uptake transporter in the same manner as it inhibits a NE uptake transporter. The inhibition of the choline transporter by hypothermia may have hampered the replenishment of the available pool of ACh and thereby contributed to the suppression of the stimulation-induced ACh release.

Limitations

In *protocol 1*, because we did not measure the infarct size in the present study, the degree of myocardial protection by hypothermia was undetermined. Whether the reduction of ischemia-induced neurotransmitter release correlates with the reduction of infact size requires further investigations. In *protocols 2* and *3*, baseline NE and ACh levels were not measured. The reduction of stimulation-induced NE and ACh release by hypothermia might be partly due to the reduction of baseline NE and ACh levels. However, because transection of the stellate ganglia (31) or vagi (3) reduces the baseline NE and ACh levels, changes in the baseline NE and ACh levels by hypothermia in *protocols 2* and *3* could not be as large as those observed under innervated conditions in *protocol 1* (Figs. 1 and 2).

In conclusion, hypothermia attenuated the ischemia-induced releases of NE and ACh in the ischemic region to ~30 and 20% of those observed under normothermia, respectively. Hypothermia also attenuated the nerve stimulation-induced releases of NE and ACh to ~70% of those observed during normothermia. In contrast, hypothermia did not affect the decreasing response in the NE level and the increasing response in the ACh level in the nonischemic region, suggesting that the Bezold-Jarisch reflex evoked by the LAD occlusion was maintained.

GRANTS

This study was supported by Health and Labour Sciences Research Grant for Research on Advanced Medical Technology, Health and Labour Sciences Research Grant for Research on Medical Devices for Analyzing, Supporting and Substituting the Function of Human Body, and Health and Labour Sciences Research Grant H18-Iryo-Ippan-023 from the Ministry of Health, Labour and Welfare of Japan; Program for Promotion of Fundamental Studies in Health Science from the National Institute of Biomedical Innovation; a grant provided by the Ichiro Kanehara Foundation; Ground-based Research Announcement for Space Utilization promoted by the Japan Space Forum; and Industrial Technology Research Grant Program 03A47075 from the New Energy and Industrial Technology Development Organization of Japan.

REFERENCES

1. **Akiyama T, Yamazaki T.** Norepinephrine release from cardiac sympathetic nerve endings in the in vivo ischemic region. *J Cardiovasc Pharmacol* 34: S11–S14, 1999.

2. **Akiyama T, Yamazaki T, Ninomiya I.** In vivo monitoring of myocardial interstitial norepinephrine by dialysis technique. *Am J Physiol Heart Circ Physiol* 261: H1643–H1647, 1991.
3. **Akiyama T, Yamazaki T, Ninomiya I.** In vivo detection of endogenous acetylcholine release in cat ventricles. *Am J Physiol Heart Circ Physiol* 266: H854–H860, 1994.
4. **Chernow B, Lake CR, Zaritsky A, Finton CK, Casey L, Rainey TG, Fletcher JR.** Sympathetic nervous system "switch off" with severe hypothermia. *Crit Care Med* 11: 677–680, 1983.
5. **Damsma G, Fibiger HC.** The effects of anaesthesia and hypothermia on interstitial concentrations of acetylcholine and choline in rat striatum. *Life Sci* 48: 2469–2474, 1991.
6. **Duncker DJ, Klassen CL, Ishibashi Y, Herrlinger SH, Pavek T, Bache R.** Effect of temperature on myocardial infarction in swine. *Am J Physiol Heart Circ Physiol* 270: H1189–H1199, 1996.
7. **Genth K, Hofmann M, Hofmann M, Schaper W.** The effect of β-adrenergic blockade on infarct size following experimental coronary occlusion. *Basic Res Cardiol* 76: 144–151, 1981.
8. **Gerevich Z, Tretter L, Adam-Vizi V, Baranyi M, Kiss JP, Zelles T, Vizi ES.** Analysis of high intracellular [Na^+]-induced release of [^{3}H]noradrenaline in rat hippocampal slices. *Neuroscience* 104: 761–768, 2001.
9. **Hale SL, Kloner RA.** Myocardial temperature in acute myocardial infarction: protection with mild regional hypothermia. *Am J Physiol Heart Circ Physiol* 273: H220–H227, 1997.
10. **Jang IK, Van de Werf F, Vanhaecke J, De Geest H.** Coronary reperfusion by thrombolysis and early beta-adrenergic blockade in acute experimental myocardial infarction. *J Am Coll Cardiol* 14: 1816–1823, 1989.
11. **Kakinuma Y, Ando M, Kuwabara M, Katare RG, Okudela K, Kobayashi M, Sato T.** Acetylcholine from vagal stimulation protects cardiomyocytes against ischemia and hypoxia involving additive nonhypoxic induction of HIF-1α. *FEBS Lett* 579: 2111–2118, 2005.
12. **Kao LS, Westhead EW.** Temperature dependence of catecholamine secretion from cultured bovine chromaffin cells. *J Neurochem* 43: 590–592, 1984.
13. **Kawada T, Yamazaki T, Akiyama T, Sato T, Shishido T, Inagaki M, Takaki H, Sugimachi M, Sunagawa K.** Differential acetylcholine release mechanisms in the ischemic and non-ischemic myocardium. *J Mol Cell Cardiol* 32: 405–414, 2000.
14. **Kawada T, Yamazaki T, Akiyama T, Shishido T, Inagaki M, Uemura K, Miyamoto T, Sugimachi M, Takaki H, Sunagawa K.** In vivo assessment of acetylcholine-releasing function at cardiac vagal nerve terminals. *Am J Physiol Heart Circ Physiol* 281: H139–H145, 2001.
15. **Kitagawa H, Akiyama T, Yamazaki T.** Effects of moderate hypothermia on in situ cardiac sympathetic nerve endings. *Neurochem Int* 40: 235–242, 2002.
16. **Kitagawa H, Yamazaki T, Akiyama T, Mori H, Sunagawa K.** Effects of moderate hypothermia on norepinephrine release evoked by ouabain, tyramine and cyanide. *J Cardiovasc Pharmacol* 41: S111–S114, 2003.
17. **Ku DD, Lucchesi BR.** Effects of dimethyl propranolol (UM-272; SC-27761) on myocardial ischemic injury in the canine heart after temporary coronary artery occlusion. *Circulation* 57: 541–548, 1978.
18. **Kurz T, Richardt G, Hagl S, Seyfarth M, Schömig A.** Two different mechanisms of noradrenaline release during normoxia and simulated ischemia in human cardiac tissue. *J Mol Cell Cardiol* 27: 1161–1172, 1995.
19. **Lameris TW, de Zeeuw S, Alberts G, Boomsma F, Duncker DJ, Verdouw PD, Veld AJ, van den Meiracker AH.** Time course and mechanism of myocardial catecholamine release during transient ischemia in vivo. *Circulation* 101: 2645–2650, 2000.
20. **Lameris TW, de Zeeuw S, Duncker DJ, Alberts G, Boomsma F, Verdouw PD, van den Meiracker AH.** Exogenous angiotensin II does not facilitate norepinephrine release in the heart. *Hypertension* 40: 491–497, 2002.
21. **Maxwell MP, Hearse DJ, Yellon DM.** Species variation in the coronary collateral circulation during regional myocardial ischaemia: a critical determinant of the rate of evolution and extent of myocardial infarction. *Cardiovasc Res* 21: 737–746, 1987.
22. **Rona G.** Catecholamine cardiotoxicity. *J Mol Cell Cardiol* 17: 291–306, 1985.
23. **Schwartz JH.** Neurotransmitters. In: *Principles of Neural Science* (4th Ed.), edited by Kandel ER, Schwartz JH, Jessell TM. New York: McGraw-Hill, 2000, p. 280–297.
24. **Schömig A, Kurz T, Richardt G, Schömig E.** Neuronal sodium homeostasis and axoplasmic amine concentration determine calcium-independent noradrenaline release in normoxic and ischemic rat heart. *Circ Res* 63: 214–226, 1988.
25. **Simkhovich BZ, Hale SL, Kloner RA.** Metabolic mechanism by which mild regional hypothermia preserves ischemic tissue. *J Cardiovasc Pharmacol Ther* 9: 83–90, 2004.
26. **Toombs CF, Wiltse AL, Shebuski RJ.** Ischemic preconditioning fails to limit infarct size in reserpinized rabbit myocardium. Implication of norepinephrine release in the preconditioning effect. *Circulation* 88: 2351–2358, 1993.
27. **Torr S, Drake-Holland AJ, Main M, Hynd J, Isted K, Noble MIM.** Effects on infarct size of reperfusion and pretreatment with β-blockade and calcium antagonists. *Basic Res Cardiol* 84: 564–582, 1989.
28. **Van den Doel MA, Gho BC, Duval SY, Schoemaker RG, Duncker DJ, Verdouw PD.** Hypothermia extends the cardioprotection by ischaemic preconditioning to coronary artery occlusions of longer duration. *Cardiovasc Res* 37: 76–81, 1998.
29. **Vander Heide RS, Schwartz LM, Jennings RB, Reimer KA.** Effect of catecholamine depletion on myocardial infarct size in dogs: role of catecholamines in ischemic preconditioning. *Cardiovasc Res* 30: 656–662, 1995.
30. **Vizi ES.** Different temperature dependence of carrier-mediated (cytoplasmic) and stimulus-evoked (exocytotic) release of transmitter: a simple method to separate the two types of release. *Neurochem Int* 33: 359–366, 1998.
31. **Yamazaki T, Akiyama T, Kitagawa H, Takauchi Y, Kawada T, Sunagawa K.** A new, concise dialysis approach to assessment of cardiac sympathetic nerve terminal abnormalities. *Am J Physiol Heart Circ Physiol* 272: H1182–H1187, 1997.
32. **Zheng F, Kidd C, Bowser-Riley F.** Effects of moderate hypothermia on baroreflex and pulmonary chemoreflex heart rate response in decerebrate ferrets. *Exp Physiol* 81: 409–420, 1996.